Phase-resetting Responses in *Clock* Null Mutant Mice

Vinhfield X. Ta

Program in Biological Sciences
Northwestern University
Evanston, Illinois

May 7, 2007

Joseph S. Takahashi
Senior Thesis Advisor

Jason L. Chong
Research Supervisor

Phase-resetting Responses in *Clock* Null Mutant Mice

Author: Vinhfield X. Ta
Senior Thesis Advisor: Joseph S. Takahashi
Research Supervisor: Jason L. Chong

Abstract

While environmental cues such as light help synchronize the internal circadian clock of mammals to 24 hours, a core biological mechanism maintains the endogenous period near 24 hours in the absence of such light cues. A mutation in the *Clock* gene causes behavioral circadian period-lengthening and arrhythmicity when mice are placed in constant darkness. Experimental data further show that *Clock* mutants exhibit different light-induced phase-resetting responses, which can be explained by a reduction in the amplitudes of *mPer1* and *mPer2* expression, which are also important core circadian genes. However, the mutant *Clock* allele behaves as an antimorph, interfering with wild-type *Clock*, and so does not reflect a null allele. Therefore, we predicted that phase-resetting responses might also be different in the absence of *Clock* expression. To test this, we have studied a strain of mice with a *Clock* gene-trap insertion. Molecular and functional evidence shows that the gene-trap blocks *Clock* gene expression. To describe the phase-resetting response of *Clock* gene-trap mice, we exposed mice that had been kept in constant darkness to 6-hour light pulses. Using wheel-running activity to evaluate circadian rhythmicity, we show that null *Clock* expression enhances the phase-resetting effect of light. Behavioral analysis and characterization of the phase-resetting response helps us to further understand the relative importance of role of the *Clock* gene in the core circadian oscillator.

Table of Contents

Introduction **3**

Materials and Methods **17**

- Generation of Gene-trap Mouse Colonies 17
- Animals 18
- RT-PCR for Clock Gene-trap Expression 18
- Genomic Location of the Clock Gene-trap 19
- Genotyping of Clock Gene-trap Mice 20
- Genotyping of Clock Point-Mutant Mice 21
- Wheel Running Experiments 22
- Light-Dark Entrainment and Light-Pulse Experiments 22
- Analysis of Activity Records 23

Results **24**

- Molecular Evidence of Clock Gene-trapping 24
- Functional Evidence of Clock Gene-trapping 29
- Behavioral Circadian Rhythmicity in Constant Darkness 32
- Phase-Response to Light 34
- Behavioral Circadian Rhythmicity in Constant Light 42

Discussion **43**

Acknowledgments **50**

References **51**

Introduction

Circadian rhythms are manifest in outward behavioral cycles of animals, like sleep-wake cycles (1, 2), but are widespread throughout all phyla and are exhibited in many forms at the molecular, cellular, physiological, and behavioral levels (2, 3). Even the cyanobacterium *Synechococcus*, for instance, shows circadian rhythmicity in its photosynthetic machinery (3, 4), while the dinoflagellate *Gonyaulax* shows bioluminescent rhythmicity (2, 3). Biological circadian rhythms are defined as nearly 24-hour rhythms produced by an endogenous pacemaker system, or clock, which can respond and align to particular periodic phenomena from the environment, but which can also persist without such cues (3). Keeping time by an endogenous circadian clock is important for individuals or populations of a species because it contributes to their survival, by allowing them to optimize the time of activity according to environmental cycles, to anticipate events before external cues appear, and to maintain rhythmicity in the absence of environmental cues (3).

There are three reasons why understanding the circadian cycle is important. In an ecological sense, it is important toward understanding how circadian behaviors confer survival. Next, study of the underlying circadian mechanism reveals how circadian rhythmicity is generated and how its period and phase are adjusted. Such an understanding can expose the fundamental cause of problems associated with circadian timing, such as jet lag, and reveal possible treatments for them (1). Also, studying the circadian mechanism is important because evidence is emerging for mammals that the circadian cycle can be coupled to or control other important biological processes such as the cell cycle, heme biosynthesis, and bone remodelling (2, 5, 36-38). Finally, from a clinical perspective, the study of circadian periodicity provides valuable understanding towards the importance of treatment timing, since studies have shown the relevance of the time-of-day on the efficacy of drugs administered to cancer patients (39).

The present study focuses on the second of these objectives, which is to help elucidate the roles of the interacting components of the circadian pacemaker. In particular, we are interested

in the mammalian circadian clock, and to this end, we have studied the house mouse, *Mus musculus*, as the primary model organism. At the behavioral level, circadian behavior is evident in the mouse's wheel-running activity, which mimics foraging behavior in nature (3). This is demonstrated in the laboratory by the way activity is robustly limited to the dark phases of a 24-hour light-dark cycle, which we commonly call nocturnal behavior. Moreover, this activity rhythm persists with a nearly 24-hour period after light cues are removed by keeping the mice in constant darkness (2, 3, 6-9). Wheel-running activity is therefore an appropriate though indirect measure of mouse circadian behavior. Also, it is useful in the laboratory because it is easy to measure, noninvasive, and quantifiable (3). At the other end, light is known to be a cue for circadian rhythmicity because mice entrain strongly to light. For true entrainment, the animal must first have the same period as the periodic environmental cue during entrainment (3). This is evident for mice entrained to a 24-hour light-dark cycle, in which activity rhythms are confined to the 12-hour dark phase. Secondly, once the entraining cue is removed and constant conditions are established, the circadian phase must be determined by the phase during entrainment (3). This is true for mice that are moved from a light-dark cycle to constant darkness, as shown in Figure 1. Mice can also entrain to other cues besides light, including temperature and food availability (10, 11). However, light is the most potent cue and the most important since all mammals and probably all other organisms can entrain to it (2). Altogether then, rhythmic wheel-running activity is a circadian output behavior under the control of a light-responsive clock, which is to say that the mouse is a good experimental model.

To describe the circadian rhythm, a distinction is made between Zeitgeber time and circadian time (2). Both are measures of a 24-hour period. However, Zeitgeber time (ZT), which derives from "time giver" in German, refers to any daily environmental cue, especially light, to which the circadian clock can synchronize by entrainment. In the laboratory, the light-dark 12:12 cycle (LD12:12, or just LD) consists of a 12-hour light (L12) phase followed by a 12-hour dark (D12) phase. By convention, the L12 phase begins at ZT0 (hour zero in ZT) and the D12 phase at ZT12 (hour twelve in ZT). In contrast, circadian time (CT) refers to the daily

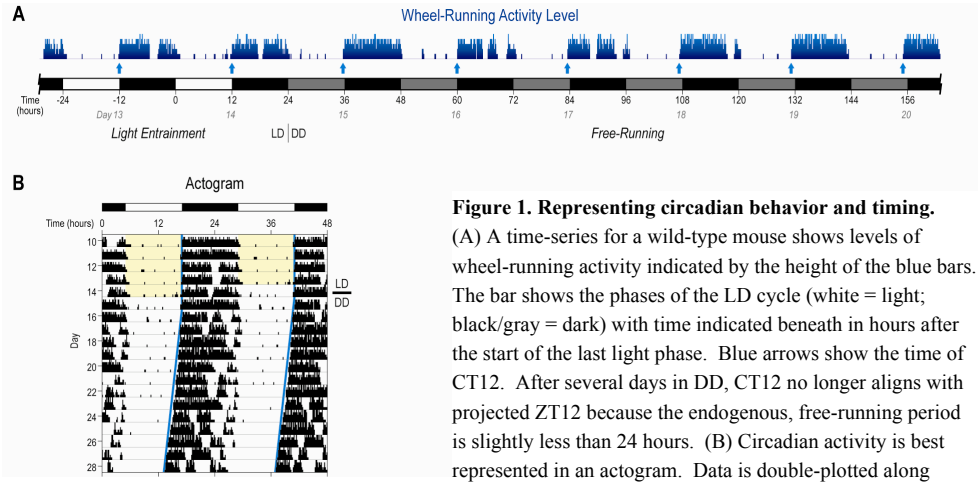

Figure 1. Representing circadian behavior and timing. (A) A time-series for a wild-type mouse shows levels of wheel-running activity indicated by the height of the blue bars. The bar shows the phases of the LD cycle (white = light; black/gray = dark) with time indicated beneath in hours after the start of the last light phase. Blue arrows show the time of CT12. After several days in DD, CT12 no longer aligns with projected ZT12 because the endogenous, free-running period is slightly less than 24 hours. (B) Circadian activity is best represented in an actogram. Data is double-plotted along 48-hour periods. In the same mouse from Fig. 1A, activity onset occurs earlier each day after Day 15, indicating a <24-hour free-running period. The light/dark bar corresponds to the LD cycle, and the day of the switch from LD to DD is indicated at the right. The yellow background here indicates exposure to light. Blue lines approximate CT12.

rhythm of the organism or animal. For the wheel-running activity cycles of laboratory mice, activity begins at CT12 by convention. This is a useful reference point because it allows the phase of the circadian rhythm to be tracked. When the mice are exposed to LD conditions, their circadian clock normally aligns to the light cue, in which case activity begins near the time of "lights off" at ZT12, and therefore CT is aligned with ZT. For this reason, CT0–12 is also called subjective day and CT12–24 subjective night. When the mice are exposed to constant conditions, especially constant darkness (DD), environmental time-giving cues are absent and the endogenous circadian clock is said to free-run. In this case, the period of CT is not necessarily 24 hours, but CT is still normalized to a "24-hour" circadian time period (*i.e.* the CT cycle still ends at CT24 even if the period length is more or less than 24 hours).

In mammals, circadian rhythms are controlled at the genetic and molecular level by a core circadian oscillator within the cell (reviewed in refs. 6 and 7). It maintains a stable period of about 24 hours even in the absence of periodic inputs from the environment of the cell or

animal. The core oscillator is comprised of the following genes and their protein products: *Clock*; *Brain, Muscle Arnt-like-1* (*BMAL1*); the mouse period (*mPer*) genes *mPer1* and *mPer2*; the mouse cryptochrome (*mCry*) genes *mCry1* and *mCry2*; and *Rev-erbα*. *Clock* and *BMAL1* encode the CLOCK and BMAL1 protein transcription factors, respectively, which both contain the basic helix-loop-helix (bHLH) and the Period-Arnt-Single-minded (PAS) domains. In the current model, CLOCK and BMAL1 proteins heterodimerize via their PAS domains, and subsequently translocate into the nucleus. There, the CLOCK:BMAL1 heterodimer binds to E-box enhancer elements of targeted genes and recruits co-activators in order to activate transcription. Many genes with circadian oscillatory expression are regulated in this way, and among them are all of the other genes belonging to the core circadian oscillator. CLOCK:BMAL1-activated transcription of *mPer1*, *mPer2*, *mCry1*, and *mCry2* leads to their respective protein products, PERs and CRYs, in the cytoplasm, where they form heteromultimeric complexes. After translocation into the nucleus, the PER-CRY complexes inhibit transcriptional activation by the CLOCK:BMAL1 heterodimer mostly through interaction between CRY and CLOCK or BMAL1. This may in turn repress histone acetyl transferase (HAT) activity. As a result, PER and CRY down-regulate their own expression, therefore forming an autoregulatory, negative feedback loop. Active CLOCK:BMAL1 heterodimers are restored following PER and CRY protein turnover. The circadian oscillator also involves a secondary, positive feedback loop, beginning with CLOCK:BMAL1-activated transcription of *Rev-erbα*. The resulting REV-ERBα protein inhibits transcription of *BMAL1* by binding the retinoic-acid related orphan receptor (ROR) response element in its promoter. Since BMAL1 also up-regulates CRY, and CRY represses CLOCK:BMAL1-mediated transcription of *Rev-erbα*, there is de-repression of *BMAL1* transcription. While the main oscillatory mechanism explained here is transcriptional, it should be noted that post-translational regulation also plays a role. This includes phosphorylation and dephosphorylation events. Nevertheless, because the role of transcription is important, experiments can demonstrate 24-hour oscillations in the mRNA levels of *BMAL1*, *mPer*, and *mCry*. With this autoregulatory oscillator in place,

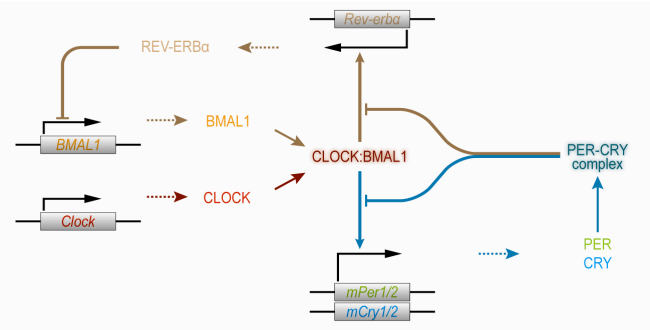

Figure 2. A current, simplified model of the mammalian core circadian oscillator. Components along the blue lines are involved in the autoregulatory, negative feedback loop, while components along brown lines are involved in the positive feedback loop.

components of the core circadian clock can drive expression of downstream targets in tempo with the rhythm of the circadian oscillator.

The many experiments that have helped to elucidate this model have also demonstrated which components are necessary. For instance, mice retain rhythmicity in constant darkness when either *mPer1* or *mPer2* is knocked out, but rapidly become behaviorally arrhythmic in constant darkness when both are knocked out (12, 13). Therefore at least one of these period genes is necessary for circadian oscillation, and both are essential for normal, or wild-type, oscillation, since knockout of either gene alters the period of the rhythm (12, 13). Similar results are observed for knockouts of the *mCry1* and *mCry2* genes (15-17). It has been noted that a third homologous period gene, *mPer3*, is not essential to the core circadian oscillator (13, 14). More relevant to the present study, a recent study has shown that *Clock* null mutants, *i.e.* mice that do not express CLOCK, also retain circadian wheel-running rhythmicity in constant darkness, suggesting that *Clock* is not necessary for mere rhythmic behavioral oscillations (18). This result is repeated in this study, and so more will be explained later. Lastly, it is highly likely that a paralog of *Clock*, currently named *Npas2*, serves as a compensating transcription factor in the absence of *Clock* in the SCN (2, 18, 46). Other studies have shown that *Npas2* forms the transcriptional partner of *Bmal1* in the mouse forebrain (47).

While the molecular components of the core circadian clock are expressed in many cells of the body, a master circadian pacemaker located in the suprachiasmatic nuclei (SCN) controls these peripheral clocks (1, 2). The SCN is located in the anterior hypothalamus, and each bilateral half of the SCN consists of a cluster of 8,000 to 10,000 neural cells (1, 2, 19). The role of the SCN is confirmed by experiments employing lesion and transplantation of the SCN (20, 21). Recipient mice or hamsters take on the circadian characteristics of the donated SCN, regardless of the genotype of the animals. Furthermore, SCN neurons show enriched expression of the circadian genes (7). And they exhibit robust circadian rhythms that are synchronized with each other in an intact SCN, but still apparent in isolation (2, 22). Peripheral tissues can also express circadian rhythmicity, even in the absence of the SCN (1, 2). For instance, *ex vivo* cell cultures of lung and liver tissue show robust though dampening oscillations (23). Nevertheless, in vivo peripheral clocks align to the master clock in the SCN (1, 2). Therefore, the SCN is more aptly a circadian pacemaker than a circadian driver (2). Circadian timing from the SCN is transmitted to other parts of the brain and to peripheral tissues via neural and humoral pathways (2). The effect is the crucial synchronization of life-sustaining activities such as sleep and wheel-running (1-3), which are consequently indicators of rhythmicity.

The role of the SCN in mammals is underscored by the fact that it bridges the body with photic input received directly from the retina (2). This is important since the circadian rhythm entrains strongly to light, and the retina is the only gateway for light-input in mammals (2). Besides the well-known rods and cones, recent work has pointed to the chronobiological importance of retinal ganglia that contain the light-sensitive pigment melanopsin (24-26). Light input from these ganglia is directly transmitted via the retinohypothalamic tract (RHT) to the SCN (2, 24). There, transduction of light-input into the phosphorylation of CRE-binding protein (CREB) allows phosphorylated CREB to bind the cAMP responsive element (CRE) in the promoter of *mPer1* and *mPer2*. Transcription of these genes is consequently activated, independent of CLOCK:BMAL1-mediated activation. Other mechanisms such as chromatin remodeling may also help increase *mPer* expression (1). The result is that light can induce

expression of *mPer1* and *mPer2*, especially when *mPer* mRNA levels are normally low, *e.g.* in a trough during subjective night (9, 27-30). In contrast to the period genes, light does not appear to directly induce expression of the cryptochrome genes (1). Since the mPERs participate in the core oscillator, light has a complete pathway for affecting the circadian rhythm. The rhythm is then propagated from the SCN, so that activity, including wheel-running, synchronizes with the phase of the master circadian clock.

The SCN is therefore responsible for entrainment to natural light-dark cycles. Light-responsiveness is valuable because the endogenous clock often has a period different from 24 hours and the lengths of the light and dark phases change according to season and latitude (2, 3). However, response to light allows animals to reset or entrain the phase of their circadian clock to match the environment. This phase-resetting response is the focus of the present study. In the laboratory, wild-type, C57BL/6J-strain mice free-run with a period of 23.7 hours; this reflects their endogenous clock (6-9, 18). But exposure to a 24-hour LD cycle, *i.e.* light entrainment, causes the mice to synchronize their rhythm to the LD cycle and effectively lengthen their rhythmic period to exactly 24 hours. Upon re-entrainment to the LD cycle from DD, the circadian rhythm of the mouse in DD may not already align in phase with the final light-entrained rhythm. In such a case, entrainment to light requires a shift in the circadian phase, *i.e.* phase-resetting to the new circadian cue. Consequently, light is important for both adjusting the circadian period and phase. Notably, the phase response can be rapid and sensitive, meaning the new circadian phase will be set after just one LD cycle or a short pulse of light (9). On the other hand, transient shifts to the new phase can be observed over the course of a few days (3).

The mechanism for light-induced phase-resetting involves the RHT and PER-induction pathways already described. At the molecular level, induction of *mPer1* and *mPer2* can cause their transcript levels to rise out of phase with the old rhythm (27-29). If induction is strong enough, the rhythm will be reset according to the light-induced *mPer* levels (3). The circadian phase is thereby shifted positively or negatively, which corresponds to a phase advance or delay,

respectively. Consequently, examining the transcript levels of *mPer1* and *mPer2* provides the most information about the circadian response to light.

It is also important to understand both the wild-type oscillation and the effect of light-pulsing on *mPer1* and *mPer2* transcript levels. Experiments show that in LD, *mPer1* levels peak at CT6 and *mPer2* at CT9. In DD, *mPer1* still peaks at CT6, while *mPer2* peaks at CT8 (29). Furthermore, the level of *mPer* induction depends on at least three factors: the time of light-exposure, the duration of the light-pulse, and the intensity of the light. It has been reported that *mPer1* induction is strong at the beginning and end of the subjective night (28), while *mPer2* is strong at the beginning and weak at the end (31). Moreover, when mice were light-pulsed at CT17 (middle of subjective night), *mPer1* induction peaked after a 1-hour light-pulse but was minimal after a 6-hour light-pulse. In contrast, *mPer2* induction peaked after a 3-hour light-pulse but was strong even after a 6-hour light-pulse (90). Finally, light-pulses with stronger intensity can elicit stronger response patterns (3).

To study light-induced phase-resetting experimentally, light-pulses are administered to many animals that have been maintained in DD (2, 3). Using the time of CT12 (*i.e.* the onset of wheel-running activity) to mark the circadian phase, the phase-shift is determined by the difference between the phases of the circadian rhythm before and after the light-pulse. This is then related to the CT of the light-pulse. Two useful ways to understand the phase-response are the phase-response curve (PRC) and the phase-transition curve (PTC). In the PRC, the phase-shift is plotted against the CT of the onset of the light-pulse. It should be noted that since CT is used, all times are adjusted to the period of each individual animal. The PRC makes noticeable that wild-type animals are less responsive to light-pulses during the subjective day. This region, called the dead zone (3), reflects the circadian time when *mPer* levels are normally high and when light present is during entrainment (28, 29). Furthermore, light exposure in the early subjective night tends to cause phase delays, while exposure in the late night causes phase advances. This is practical for entrainment to environmental light cues, since light at late subjective night means the phase must be pulled back while light at early subjective night means

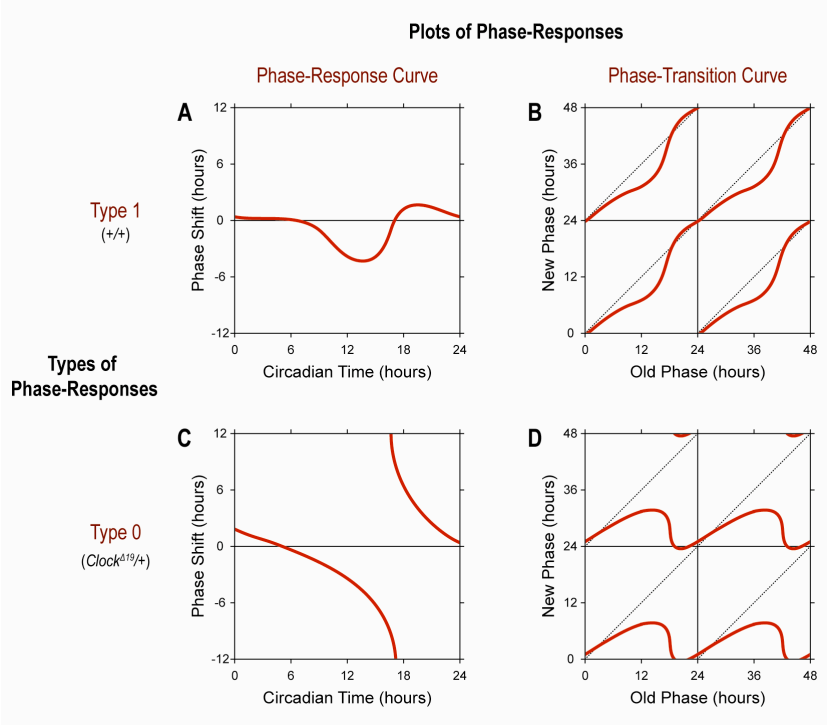

Figure 3. Models of the light-induced phase-response.
Phase response curves (PRCs; A and C) and phase transition curves (PTCs; B and D) representing Type 1 and Type 0 responses. In each PTC, both axes are double-plotted. These curves are representative of the data obtained by Vitaterna *et al.* (2006), with wild-type (A and B) exhibiting Type 1 responses and *Clock*$^{\Delta 19}$/+ (C and D) exhibiting Type 0 responses. The phase-response breakpoint for *Clock*$^{\Delta 19}$/+ mice occurs at CT17.

the phase must be pushed forward (3). Moreover, phase-delays are usually stronger for clocks whose free-running period is less than 24 hours, permitting exposure to light in the early subjective night to lengthen the photo-entrained period (3). Two types of phase-responses are evident in PRCs: Type 1 resetting and Type 0 resetting (3). In Type 1 resetting, the phase-response curve is continuous, while in Type 0 resetting, a breakpoint or discontinuity between advances and delays appears in the middle of subjective night, at about CT18. These two types of resetting are even more apparent in the PTC. The PTC compares the new, or reset, circadian phase against the initial phase. For Type 1 resetting, the average slope on the PTC is 1 (hence the name), corresponding to a diagonal line. This shows that despite the CT of the light pulse

and any phase-shifting, the new phase is nearly the same as the old phase. On the other hand, Type 0 resetting produces an average slope of 0. This indicates that phase-shifting resets the rhythm to the same phase despite the CT of the light-pulse. Generally, Type 1 indicates a weak resetting response while Type 0 reflects a strong response (3).

For this experiment, we were interested in studying the phase-resetting response in a *Clock* null mouse. After all, *Clock* participates in the core circadian mechanism and should in some way affect how the clock is reset by light. When this project was started around the summer of 2005, a *Clock* null mouse had not yet been reported, even though *Clock* had been identified as a circadian gene for over 10 years by the Takahashi group (6). This is due in part to the discovery that the mutant allele that was originally used to identify the *Clock* locus does not behave as a null allele (8). Since this study focuses on the *Clock* gene, its discovery by the Takahashi group will be elaborated.

Clock was first discovered through a forward genetic approach utilizing mutagenesis with *N*-ethyl-*N*-nitrosourea (ENU) (6). Phenotypic screens of mouse progeny led to the identification of a line of mice with mutant circadian behavior. This mutation segregated as a single, autosomal locus. While wild-type mice have a free-running period of 23.7 hours, a period of 24.5 hours was observed for heterozygous mutants, and 27–28 hours for homozygous mutants, which eventually became arrhythmic in constant darkness. The mutant allele therefore behaved semidominantly. Notably, the mutation originated and was maintained, *i.e.* backcrossed, in a coisogenic C57BL/6J background strain. The *Clock* locus was subsequently mapped to mouse Chromosome 5 (6-8, 32).

Characterization of the *Clock* locus and the wild-type and mutant alleles has provided important information. Genomic DNA and cDNA sequencing revealed that the *Clock* gene spans about 100 kilobase pairs and encodes a transcript containing 24 exons (numbered 1a, 1b and 2 through 23) (7). Importantly, the length of intron 2-3 is greater than 29 kilobase pairs (33), and the ATG translation initiation codon is found in a Kozak consensus sequence in exon 4 (7). Therefore, the first four exons belong to the 5′-UTR. By homology of the predicted amino acid

sequence, the wild-type CLOCK protein was revealed to contain an N-terminal bHLH–PAS domain and a C-terminal glutamine-rich domain (7). Finally, alternatively spliced mRNAs with or without exon 18 and either exon 1a or 1b were identified (7). Sequencing of the *Clock* mutant allele identified a point mutation, as expected from the ENU-induced mutagenesis screen (6, 7). The mutation is an A→T transversion in the 5′ splice donor site of intron 19, and causes exon 19 (immediately upstream) to be spliced out of *Clock* mRNA, without a reading frame shift (7). This results in the deletion of 51 amino acids in the glutamine-rich domain, potentially disrupting the CLOCK transactivation domain (7). Hence, the *Clock* mutant allele generated by ENU mutagenesis is here denoted by $Clock^{\Delta 19}$; the wild-type allele is labeled +.

Further experiments revealed $Clock^{\Delta 19}$ behaves as an antimorph (8). To determine this, complementation tests were performed against a strain (C3HeB) with the W^{19H} chromosomal deletion, which involves the region on Chromosome 5 that includes the *Clock* locus among others. As a result, the deletion provided a *Clock* null allele with which to perform allelomorph analysis as described by Muller (34). Progeny from the crosses had a C3H×(BALB×C57BL/6J) hybrid background. The resulting wild-type *Clock* hemizygotes ($+/W^{19H}$) showed a free-running period of 23.7 hours, which was indistinguishable from the 23.6-hour period of wild-type mice. This suggested that the null allele is recessive to wild-type. However, mutant *Clock* hemizygotes ($Clock^{\Delta 19}/W^{19H}$) exhibited a period of 25.6 hours, with mildly disrupted activity rhythms. In contrast, *Clock* heterozygotes ($Clock^{\Delta 19}/+$) exhibited a period of 24.2 hours. This 1.4-hour difference is significant, and shows that if the wild-type allele is present, it antagonizes the mutant allele, effectively abating the period-lengthening defect of $Clock^{\Delta 19}$. As a result, the *Clock* mutant allele is not a null allele, and the mutant period-lengthening phenotype is due to the dominant negative effect of the mutant allele, not to the lack of wild-type *Clock*. This antimorphic behavior is reasonable considering that mutant CLOCK retains the bHLH–PAS domain but not its transactivation domain (7). Unfortunately in this study, a homozygous *Clock* null could not be generated using the W^{19H} deletion, because the deletion was homozygous lethal (probably due to other deleted genes in the region besides *Clock*) (8). A third study further

confirms the involvement of the *Clock* gene and the behavior of $Clock^{\Delta 19}$ in the mutant phenotype (32). In this study, transgenic overexpression of a BAC clone containing the *Clock* gene rescued *Clock* mutant mice by restoring the wild-type period. This shows that overexpressed wild-type CLOCK can outcompete the mutant protein to restore wild-type function, which is expected of the antimorphic behavior.

Previous research in the Takahashi laboratory (9) has additionally shown that *Clock* expression can affect the light-induced phase-response. In the study, phase-resetting curves were constructed for *Clock* wild-types and $Clock^{\Delta 19}$ heterozygotes in a C57BL/6J-strain background. Six-hour light pulses were administered because the wild-type mice responded more strongly and with lower variance in phase-shift magnitude. The PRCs and PTCs showed clear Type 0 resetting for heterozygotes, while wild-type mice showed Type 1 resetting, as represented in Figure 3. Of note, phase delays in wild-type mice were generally greater in magnitude than phase advances but still less than 6 hours. On the other hand, the strong light response in heterozygotes caused nearly 12-hour phase-shifts near CT17. Also, their Type 0 response was characterized by phase-resetting between CT0 and CT8. Similar curves could not be constructed for $Clock^{\Delta 19}$ homozygotes because their arrhythmic behavior in DD precluded determination of their pre-light-pulse circadian phase. Nevertheless, light-pulses tended to reinitiate circadian rhythmicity, and Vitaterna *et al.* were able to show that light-pulsing caused their rhythm to reset near CT6. Vitaterna *et al.* inconclusively attributed this to either a strong phase-resetting response, like that seen in $Clock^{\Delta 19}$ heterozygotes, or to re-initiation of rhythmicity. To explain stronger phase-resetting responses in general, two alternative explanations can be raised: either the amplitude of the circadian pacemaker is lower while light input is the same, or light-induced input is higher and oscillation the same. To determine both the level of light input and circadian oscillation, *mPer1* and *mPer2* mRNA levels in the SCN were measured. Apparently, the levels of light-induced *mPer1* and *mPer2* expression were not significantly different between wild-types and heterozygotes when a light-pulse was administered at CT17. On the other hand, both period genes were reported to oscillate at lower amplitude in heterozygous mutants that had been

maintained in DD for at least 3 weeks. Vitaterna *et al.* therefore concluded that the lower amplitude of circadian oscillation permitted light input to have a stronger effect in heterozygous mutants compared to wild-type mice. Interestingly, this study also showed that, unlike *mPer2*, *mPer1* mRNA levels after a 6-hour light-pulse at CT17 are not significantly higher than CT23 levels in DD. Yet $Clock^{\Delta 19}$ heterozygotes show the strongest phase-shifts when pulsed for 6 hours at CT17, suggesting that *mPer2* induction plays a stronger role in light-induced phase-resetting.

Since the $Clock^{\Delta 19}$ allele is an antimorph of the wild-type allele, the phase-resetting responses determined for $Clock^{\Delta 19}$ mutants do not necessarily reflect light-induced resetting in the absence of *Clock* expression. However, the previous study does suggest that without proper *Clock* gene and protein function (*e.g.* in the $Clock^{\Delta 19}$ homozygote), the light-induced phase-response will be different. Consequently, it would be useful to determine how a *Clock* null background affects phase-resetting behavior. Along with this, it would be important to characterize the molecular mechanism that underlies any behavior differences and to determine light-induced events such as *mPer1* and *mPer2* induction. Such analysis would provide valuable insight into the processing of light-input signals to the core circadian oscillator.

Subsequent to the start of this project in 2005, DeBruyne *et al.* from the Reppert laboratory published their findings using gene-targeted *Clock* null mice (18). In their May 2006 report, they reported using the *Cre-LoxP* system to delete exons 5 and 6 from the chromosomal Clock locus. Genetic and molecular analysis revealed that a $Clock^{\Delta 5\text{-}6}$ allele was created, and in the homozygous state, leads to null expression of CLOCK protein in both the SCN and liver. Behavioral study of the $Clock^{\Delta 5\text{-}6}$ hetero- and homozygotes revealed that CLOCK-deficient mice could maintain robust circadian rhythms in constant darkness. The $Clock^{\Delta 5\text{-}6}$ heterozygotes (heterozygous null mice) showed circadian periods similar to those of wild-types, in agreement with the King et al. (7) study. Meanwhile, even $Clock^{\Delta 5\text{-}6}$ homozygotes (null mice) maintained a period of 23.2 hours in DD, just 20 minutes shorter than wild-types. CLOCK null mice were also observed to have slightly lower activity than wild-types. At the molecular level, circadian

oscillations were reported in the SCN of *Clock* null mice. Dramatically lower amplitudes of mRNA oscillation were observed for *mPer1* and *Rev-erbα*. *BMAL1* also showed lower amplitude as well as elevated mRNA levels. On the other hand, *mPer2* mRNA levels had similar amplitude compared to wild-type mice. In addition, oscillations in effector genes of the core circadian clock were dampened in CLOCK null mice. It was concluded from these data that *Clock* is not required for robust circadian molecular and behavioral rhythmicity, although it does have some effect on circadian amplitude. More relevant to the present study, DeBruyne et al. further administered 4-hour light pulses to mice either at ZT12 or ZT20 during the subjective night. Their experiments showed that wild-type and $Clock^{\Delta 5\text{-}6}$ heterozygous mice responded similarly with phase delays when pulsed at ZT12: −1.6 hours and −1.9 hours, respectively. In contrast, $Clock^{\Delta 5\text{-}6}$ homozygotes showed no significant phase-shift. When light-pulses were administered at ZT20, the $Clock^{\Delta 5\text{-}6}$ homozygotes apparently showed much stronger phase advances (+6.8 hours) compared to wild-types (+1.8 hours) or $Clock^{\Delta 5\text{-}6}$ heterozygotes (+2.0 hours). From their experiments and data, DeBruyne *et al.* concluded that CLOCK-deficiency in mice caused weaker phase-delays and stronger phase-advances compared to wild-type mice.

While the previous study by DeBruyne *et al.* had similar goals as our project, their experimental method and conclusions do not provide accurate answers. In particular, their light-pulsing experiments were conducted by extending the light phase of the last LD cycle, from ZT12 to ZT16; or light-pulses were administered at ZT20 after the last L12 phase before release into DD (18). All mice were therefore pulsed within the first 12 hours after the last "lights out." Because the effects of the previous LD cycle are still present, the experiment did not accurately reflect light-pulsing of the endogenous, free-running clock. Furthermore, since pulsing was conducted at only two time-points, an accurate phase-resetting response could not be constructed from the data. Indeed, this study omitted demonstrating the effect of CLOCK-deficiency on phase-resetting during subjective day or the middle of subjective night, which is particularly important since Type 1 and Type 0 resetting (i.e. weak versus strong phase-response) differ most at this time. Moreover, without fully characterizing the phase-response, it was assumed that

delays would be caused by pulses at ZT12 and advances by pulses at ZT20 for all genotypes. Even more, the authors used phase-shifts at ZT12 or ZT20 to generally represent phase-delays or phase-advances, respectively. However, Figure 3 shows that this is misleading since the phase-delay at CT12 (which is similar between Types 1 and 0) is not indicative of the shift at CT17 (which is different between Types 1 and 0). In all, therefore, their results about light-induced phase-resetting in CLOCK-deficient mice are incomplete. The authors are also misleading in their conclusion because they imply that these mice are less able to respond with phase-delays. Finally, no molecular mechanism is provided to explain the behavioral results. And although the authors do demonstrate lower amplitude of oscillation of the core circadian genes in the SCN, their mRNA extractions were conducted in the cycle immediately following entrainment to LD, without a sufficient period of free-running (18). Consequently, the best conclusions that the previous study reaches is that light-responses are merely altered by CLOCK-deficiency.

Using the study by Vitaterna *et al.* (9) as a guide, we therefore sought to better describe and explain the effect of CLOCK-deficiency on light-induced phase-resetting. Our experimental design improves that used by DeBruyne *et al.* (18) in a few important ways. First, we administered light-pulses to mice free-running in DD. This allowed us to observe pre-light-pulse free-running periods and analyze phase-shifts in relation to free-running circadian time rather than Zeitgeber time. We were therefore able to construct phase-response and phase-transition curves to more completely and accurately describe the effect of CLOCK-deficiency on light-induced phase-resetting.

Materials and Methods

Generation of Gene-trap Mouse Colonies

Mouse embryonic stem (ES) cells derived from the P007F12 line were obtained from the German Gene Trap Consortium (GGTC, Germany). The P007F12 line was generated by mutation with the FlipROSAβgeo vector, a retroviral vector containing the gene-trap. The ES cells were the F1 generation of a cross between C57BL/6J and 129S6/SvEvTac genetic

backgrounds. Blastulas were obtained from pregnant embryonic-donor females. Gene-trap ES cells were then injected *in vitro*, and the blastula was reimplanted into a surrogate mother. Embryos consisting of a mix of two genetically distinct cells gave rise to chimeric mice, which were identified by mixed coat color. Seven chimeras were backcrossed to C57BL/6J mice to screen for mice in which the gene-trap ES cells had differentiated into the germ line, permitting transmission of the gene-trap allele to progeny. Founders were positively identified for gene-trap transmission by PCR genotyping and subsequently used to found our *Clock* gene-trap colonies.

Animals

The *Clock* gene-trap colony was maintained and expanded by backcrossing to C57BL/6J wild-type mice to attain second-generation (N2) heterozygotes. Backcrossing allowed us to reduce background strain effects of the original [C57BL/6J × 129S6/SvEvTac] ES cell strain. The *Clock* point-mutation allele ($Clock^{\Delta 19}$) and the *mPer2::Luc* knock-in allele have been previously generated in the Takahashi Laboratory. These alleles have been maintained together in a congenic mouse strain, which has been backcrossed to C57BL/6J for at least nine generations (N9). For the experiment, we used mice homozygous for both $Clock^{\Delta 19}$ and *mPer2::Luc*. These mice were crossed to $Clock^{Gt}$/+ heterozygotes to obtain recombinants of the *Clock* alleles. Littermates of the cross were used in the wheel-running experiments. $Clock^{Gt}$ homozygotes were obtained by intercrossing two N2 $Clock^{Gt}$ heterozygotes. Littermates were kept for wheel-running experiments. All mice were bred in the Center for Comparative Medicine (CCM) in the Pancoe-ENH Life Sciences Pavilion at Northwestern University, Evanston. For wheel-running experiments, animals were moved to the CCM facilities in the Hogan Building. All care and experimental treatment of the mice complied with guidelines established by the Institutional Animal Care and Use Committee (IACUC) at Northwestern University.

RT-PCR for Clock Gene-trap Expression

RT-PCR was used to verify post-transcriptional splicing of the putative *Clock* gene-trap

into *Clock* mRNA immediately downstream of exon 2. This was carried out using the TaqMan Reverse Transcription Reagents kit (N8080234) and protocol from Applied Biosystems (ABI). RNA was extracted from cultured P007F12 ES cells, and a 306-bp fragment containing the transcriptional splice junction between exon 2 and the gene-trap was amplified using the primers TGAAAGAAAAGCACAAGAAGAAA and TGCGCAACTGTTGGGAAG. Similar control experiments were run with the primers GAAACTTTTACAGGCGTTGTTG and GCTTACGGTAAACACCATAACACA, which were designed to amplify the 206-bp junction between exon 2 and the downstream exons 3 and 4. Amplification was detected as increasing fluorescence from SYBR Green (ABI) on the ABI 7900 Real-time PCR machine. Specific amplification was confirmed by standard DNA sequencing of the complementary DNA (cDNA) product.

Genomic Location of the Clock Gene-trap

P007F12-line genomic DNA was obtained from mouse tail clips by alkaline hydrolysis. 3–4 μg DNA was digested using Sau3A1 restriction endonuclease (New England BioLabs, NEB) in Sau3A1 buffer (NEB), diluted with double de-ionized water (ddH_2O) to a 40-μl reaction volume, for 3 hours at 37°C; this was followed by incubation at 65°C for 20 minutes to inactivate the restriction enzyme. Two oligonucleotide species (SOURCE) were used to prepare linkers called splinkerette units:
CGAAGAGTAACCGTTGCTAGGAGAGACCGTGGCTGAATGAGACTGGTGTCGACACTAGTGG and GATCCCACTAGTGTCGACACCAGTCTCTAATTTTTTTTTTCAAAAAAA. The units were prepared using 150 pmol of each oligonucleotide with NEB Buffer 2 (NEB) in a 100-μl reaction. This was incubated at 65°C for 5 minutes to permit annealing prior to the next step. The ligation reaction between the splinkerette units and digested genomic DNA consisted of 600-800 ng Sau3A1-digested tail DNA, 3 μl annealed splinkerette linkers, 400 U T4 ligase (NEB), and ligation buffer in a 20-μl reaction volume. The reaction mix was incubated overnight at 15°C, replenished with 200-U more ligase and incubated at 15°C for an additional 4 hours. DNA fragments were amplified by two PCRs run in tandem. Both PCRs used 0.4 μM of forward and

reverse primers, standard 1× PCR Buffer, 0.5 mM dNTPs, and 0.7 µl Roche cDNA Polymerase (Clontech, Lot#5110424). 1 M Betaine was added to increase amplification efficiency. Diluted DNA was added, and the final reaction volume was adjusted to 50 µl with ddH_2O. For the first round of PCR, 25 µl QIAEX II-purified DNA was added to the reaction mix, and the primers CGAAGAGTAACCGTTGCTAGGAGAGACC and GCTAGCTTGCCAAACCTACAGGTGG were used. The thermocycling profile for the first PCR was the following: 90 sec at 94°C; 2 cycles of 94°C for 1 min, 64°C for 30 sec, 68°C for 2 min; 30 cycles of 94°C for 30 sec, 64°C for 30 sec, 68°C for 2 min; and 10 min at 68°C. The second round of PCR used 5 µl of a 1:500 dilution of the first post-PCR mix, and the primers GTGGCTGAATGAGACTGGTGTCGAC and GCCAAACCTACAGGTGGGGTCTTT. The thermocycling profile for the second PCR was the following: 90 sec at 94°C; 25 cycles of 94°C for 30 sec, 65°C for 30 sec, 68°C for 90 sec; 5 cycles of 94°C for 30 sec, 60°C for 30 sec, 68°C for 90sec; and 10 min at 68°C. Products from the second PCR were separated by gel electrophoresis on a TBE, 1% agarose, 0.1% ethidium bromide gel. A standard UV spectrometer was used to visualize the gel. Identified bands were each cut from the gel and purified with the QIAEX II Gel Extraction Kit. Standard DNA sequencing was carried out using the purified DNA fragment and the same primer sequences for the second round of PCR.

Genotyping of Clock Gene-trap Mice

To obtain DNA, 0.5-cm tail clips were taken and subjected to alkaline hydrolysis; 1:100 dilutions of DNA from the extractions were used for genotyping. Polymerase Chain Reaction (PCR) was used to determine the genotype of mice at the *Clock* gene-trap locus. Mice were identified for the presence of the gene-trap using the primers AGTGACAACGTCGAGCACAG and CGGTCGCTACCATTACCAGT to amplify a 322-bp fragment internal to the gene-trap. This method was used to identify founders of the *Clock* gene-trap colony and carriers of gene-trap allele. A second method was developed to differentiate between gene-trap homozygotes and heterozygotes. Using the genomic location of the gene-trap determined above, we constructed a

second set of primers to amplify the intact portion of *Clock* intron 2-3 where the *Clock* gene-trap insert is found in the $Clock^{Gt}$ allele. As shown in Figure 4, these primers, CTTCCCATCCTCCTTTCTCC and AATCAATGCGGTGGTTTCTC, amplify a 444-bp fragment in the $Clock^{+}$ or $Clock^{\Delta 19}$ allele. Formally, these primers can produce a much larger amplicon containing the gene-trap sequence from the $Clock^{Gt}$ allele, but the efficiency of this reaction is negligible under the PCR conditions used. Notably, efficient primers could not be constructed to amplify the junction between the gene-trap and Clock intron 2-3 due to the repetitive DNA sequences at the 5′ and 3′ ends of the gene-trap insert. The following thermocyclic PCR profile was used: 2 min at 95°C; and 30 cycles of 95°C for 30 sec, 55°C for 30 sec, 72°C for 45 sec. PCR products were run on 1% agarose gels. Using both primer sets in separate reactions allowed us to distinguish among Clock wild-type, $Clock^{Gt}$ heterozygous and homozygous genotypes.

Genotyping of Clock Point-Mutant Mice

Since the $Clock^{\Delta 19}$ allele differs by a single point mutation from the $Clock^{+}$ allele, and essentially from the $Clock^{Gt}$ allele as well, standard PCR genotyping like that used to genotype the $Clock^{Gt}$ allele is insufficient for distinguishing the $Clock^{\Delta 19}$ allele. Rather, single nucleotide polymorphism (SNP)-based real-time PCR genotyping was used. This method of allelic discrimination has been used in the Takahashi laboratory and is similar to that described in ref. 35. Briefly, two reactions are run for each sample. Both use the same complimentary reverse primer, GGAACTCAAAATGTGAAAGAGATTC, but the forward primer anneals to the DNA with either a match or a mismatch at its 3′ nucleotide depending on the alleles present. The forward primer CATGGTCAAGGGCTACAGGTA anneals perfectly with wild-type *Clock*, and the alternative primer CATGGTCAAGGGCTACAGGTT anneals perfectly with $Clock^{\Delta 19}$. Mismatch of the 3′-end of the forward primer decreases amplification efficiency of the target DNA sequence, such that amplification reaches half saturation at a later PCR cycle. Both primer sets produce a 70-bp amplicon. The reactions used commercially available AmpliTAQ Gold (QIAGEN), SYBR

Green (QIAGEN) to detect amplification of double-stranded DNA, and 1:100 diluted DNA from alkaline hydrolysis, in the ABI PRISM 7900 (Applied Biosystems, Inc.) Real-time PCR machine. The real-time PCR followed this thermocyclic profile: 95° for 10 min, followed by 35 cycles of 95° for 10 sec and 56° for 10 sec.

Wheel Running Experiments

Mice were housed individually in cages equipped with stainless steel running wheels. The cages were kept in light-tight, ventilated boxes. Controlled lighting within the boxes was provided by green LED lights emitting about 100 lux, and controlled by a PC computer system running the ClockLab (Actimetrics) software. Activity was measured by rotation of the running wheel, which triggers an electronic clicker attached to the outside of the cage, such that one revolution produces one click. Data was collected and recorded as the number of revolutions in one-minute bins, by the computer software. Mice were introduced to the wheel-running experiment 1 hour before "lights-out" in order to reduce the confounding effects of introducing the mice to a new environment. During the course of the experiment, the light-tight boxes were opened only while the internal lights were on (during the light cycle or during 6-hour light pulses); or, if the internal lights were off, lights in the cage holding room were shut off and the mice were viewed with infrared viewing goggles (ANVS, Inc., Salt Lake City, Utah; Model: ANVS-3105). This was done to avoid unintended exposure of the mice to visible light. Gene-trap mice were N2 or N3. At the beginning of the experiment, all mice were 8- to 10-weeks old.

Light-Dark Entrainment and Light-Pulse Experiments

All wheel-running experiments began with entrainment of the mice to a light-dark (LD) cycle of 12 hours of light (L12) followed by 12 hours of darkness (D12), or LD12:12 cycle, for at least 14 days. Following lights-off on day 14 (or later), the mice were released into constant darkness (DD) for at least 3 weeks. After this free-running period, 6-hour light pulses were administered and succeeded by another 12 days, at minimum, of free-running in DD. Wheel-

running activity was collected throughout this time. Mice in this experiment were pulsed at most seven times, with each pulse at least 12 days apart. If mice were inadvertently exposed to light during DD, wheel-running data for phase-shifting was not analyzed, and the mice were allowed to free-run in DD for at least 12 days before administering another light-pulse.

Analysis of Activity Records

The ClockLab (Actimetrics) data analysis software was used to plot activity records, calculate circadian periodicity, and calculate the magnitude of phase-shifts. Activity is double-plotted in the actograms, such that each 24-hour day is plotted immediately to the right of and below the previous day. Calculations involved eye-fitting the time of activity onset for a certain number of days, and then drawing a least-square fit line through these times. Circadian period was determined by this least-square fit line. Overall free-running periods were fit to 28 days of steady, rhythmic activity after at least 3 weeks in DD. Free-running periods were also determined at specific weeks into DD using a 10-day interval of rhythmic activity. Period in LL was fit to 28 days after 2 weeks of constant light. The ClockLab software was also used to calculate averages of activity level and derive relative FFT power from χ^2 periodogram analyses (42) using a 28-day interval of activity in DD.

Determination of the phase-shift was similar to that described in ref. 9. One least-square fit line through activity onset was drawn using 7 days preceding the day of the light-pulse. This line was used to calculate the pre-pulse circadian period, or “old” period. Extrapolation of this line to the day of the pulse was taken as the time of CT12 relative to the preceding rhythm, or “old” CT12. The circadian time of the onset of the light-pulse was determined relative to “old” CT12 by taking the time difference between “old” CT12 and pulse onset, multiplying this difference by 24 and dividing by the “old” period. This corrects for the circadian period according to each individual mouse and expresses all time in circadian time. Likewise, a second line was drawn using the 7 days following the third day after the light-pulse. These first three days following the pulse were skipped to avoid the effects of transient phase-shifting. This line

was used to calculate the post-pulse circadian period, or "new" period. Back-extrapolation of this line to the day of the pulse was taken as the time of the "new" CT12. The phase-shift magnitude was calculated by taking the difference between the "new" and "old" CT12 times, multiplying by 24 and dividing by the "old" circadian period. For the phase-transition curves, the new circadian phase was determined by taking the time difference between the "new" CT12 and pulse onset, multiplying by 24 and dividing by the "new" period. Notably, addition of the phase-shift to the "old" phase does not always yield the "new" phase because the "old" and "new" circadian period to which the phases are adjusted may be different.

Results

Molecular Evidence of Clock Gene-trapping

Four embryonic stem (ES) cell lines were obtained from the German Gene Trap Consortium (GGTC): P007F12, A050F06, F060F06, and W174F05. For each line, a different viral vector was used to insert a gene-trap randomly into the mouse genome. The P007F12 line was transduced with the FlipROSAβ-Geo gene-trap vector, a retroviral vector that contains the *β-Geo* gene downstream from a splice acceptor and upstream from a polyadenylation signal (Figure 4A). Because *β-Geo* lacks its own promoter, *β-Geo* expression depends both on its position downstream from an endogenous, actively transcribed gene and on efficient splicing of the gene-trap into the endogenous mRNA transcript. The polyadenylation signal in the gene-trap causes premature transcriptional termination, such that downstream regions of the endogenous gene are not transcribed. Thereby proper expression of the gene is disrupted, and transcription of the upstream region is trapped. Meanwhile expression of *β-Geo* produces β-galactosidase fused to a neomycin-resistance marker. The presence of these markers is easily assayed, and provides an indication of gene-trap function. Importantly, efficiency of the gene-trap, i.e. splicing into mRNA, can be limited by positional effects, which makes it important to test gene-trap efficiency. The W174F05 line was mutated with a similar retroviral vector with *β-Geo*. For the A050F06 and F060F06 lines, the *β-Geo* gene-trap was integrated via a non-retroviral vector.

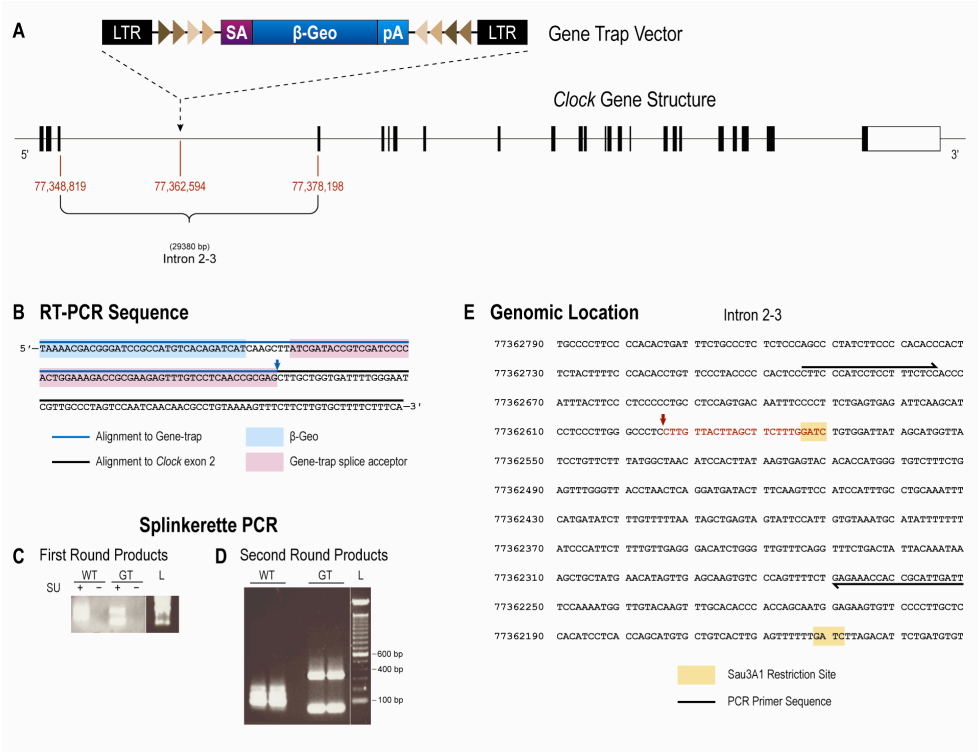

Figure 4. Insertion and expression of the *Clock* gene-trap in the P007F12 line.
Numbers indicate nucleotide position on mouse Chromosome 5, based on the Ensembl database (33). (A) The viral gene-trap vector used by the German Gene Trap Consortium (GGTC) contains the β-Geo gene with an upstream splice acceptor (SA) and downstream polyadenylation site (pA). Triangles indicate the direction and position of sites for post-insertional modification. Filled boxes in the *Clock* gene indicate exons. The unfilled white box indicates the 3′-UTR. In the P007F12 line, the gene-trap inserted into the >29kb region of intron 2-3. (B) The partial cDNA sequence of one RT-PCR experiment shows complete alignment to *Clock* exons or the gene-trap. The transcriptional template strand is shown, so that exon 2 is upstream of the gene-trap in mRNA. The expected gene-trap splice site, indicated by the blue arrow, coincides with the exonic junction. (C and D) Products from splinkerette PCR using wild-type (WT) or gene-trap-positive (GT) DNA and splinkerette units (SU), are separated by gel electrophoresis with 100-bp ladder (L). (C) Crude separation shows amplification occurred after the first round of PCR. (D) Both lanes for each genotype are from one splinkerette PCR reaction. Two distinct bands ~350-bp and <100-bp amplify for gene-trap-positive DNA, but not for WT DNA. (E) The partial genomic sequence of intron 2-3 (33). Sequencing of the <100-bp band from splinkerette PCR produced the sequence shown in red. The red arrow indicates the vector insertion site between positions and 77,362,595. Note that the intronic sequence is written 5′→3′ but the position numbers decrease, because *Clock* is on the minus strand.

The GGTC used rapid amplification of cDNA ends (RACE), a high throughput screening method, to initially identify our four ES cell lines as having a gene-trap insertion in *Clock* intron 2-3. Insertion of the gene-trap into this region was ideal for a few reasons. First, the upstream exon, exon 2, splices into all known *Clock* splice variants, and so we expected to find the gene-trap spliced immediately downstream of exon 2 in mRNA. Second, since intron 2 is located upstream from the translational start site in exon 4, an effective gene-trap in this intron would truncate transcription of *Clock* in the 5′-UTR. This would eliminate both functional *Clock* mRNA and CLOCK protein.

Once we acquired the ES cell lines, we independently verified that the gene-trap inserted downstream of exon 2 and simultaneously confirmed that the transcriptional machinery spliced the gene-trap into the *Clock* transcript. To do so, we performed reverse transcription polymerase chain reaction (RT-PCR) on a culture of ES cells to amplify the mRNA splice junction between exon 2 and the gene-trap. In a separate control experiment, the splice junction between exon 2 and exon 3 was amplified. Sequencing of the cDNA product from RT-PCR revealed alignment to both exon 2 and the 5′ end of the gene-trap for the P007F12, A050F06, and F060F06 ES cell lines (Figure 4B). Furthermore, the gene-trap was spliced precisely as predicted by the vector sequence. The cDNA sequence of the fourth ES line, W174F05, showed stronger alignment to *Utrn*, a gene located on mouse Chromosome 10, than to *Clock* (data not shown). As a result, we concluded that gene-trap insertion into *Clock* intron 2-3 was falsely identified by RACE for this cell line, and we did not use the W174F05 line for further experimentation.

Cultures of the remaining three lines were then assayed for β-galactosidase by staining with *ortho*-nitrophenyl-β-galactoside (ONPG). Cleavage of this substrate by β-galactosidase produces a visible blue dye. Saturation of the signal occurred at nearly twice the rate in the P007F12 cell line compared to the other cell lines (data not shown; experiment by J. L. Chong). Since the rate of substrate cleavage and strength of the signal are indirect measures of gene-trap reporter gene expression, this experiment suggested that the gene-trap was most efficient in the P007F12 line.

Further molecular evidence of *Clock* gene-trapping was provided by determining the positional location of the gene-trap in the mouse genome. To do so, splinkerette PCR was used to amplify any unknown genomic fragment joined to our known gene-trap sequence. Nested PCR was used in conjunction with the splinkerette method to increase specificity. Total genomic DNAs from the P007F12 line and wild-type mice were partially digested with the Sau3A1 restriction enzyme, producing 5′ GATC overhangs. Splinkerette units, which each have one 5′ GATC overhang, were then ligated to the digested ends of the genomic fragments. A region of the free 3′ end of the splinkerette linker is mismatched with the antistrand strand and is also self-complementary, resulting in a looped-back hairpin. This mismatched hairpin reduces nonspecific amplification due to "end-pair priming" during PCR (40). The total population of genomic DNA fragments with ligated splinkerette units was subjected to nested PCR, consisting of two consecutive rounds of PCR. Each reaction used one primer specific to the gene-trap vector and a second primer specific to the splinkerette linker. Before PCR begins, the linker-specific primer has no DNA template to which to hybridize. If the splinkerette reaction works perfectly, a proper template strand will arise after the first PCR cycle due to priming and elongation of the gene-trap specific primer. As a result, the fragment containing gene-trap and unknown DNA sequence has complementary sites for both primers. It can subsequently be amplified geometrically by normal PCR. Other genomic fragments lack the sites for both primers, so that exponential amplification is not possible.

To crudely test for amplification after the first round of PCR, a sample of the PCR product was separated and visualized by gel electrophoresis (Figure 4C). Amplified products were observed for both gene-trap-positive DNA and wild-type DNA, but distinct bands appeared for the former. For the second round of PCR, the first PCR product mixture was diluted 1:500 in order to reduce the amount of amplified DNA template and dilute away left over reagents and nonspecific genomic fragments, which were still present but at relatively minimal concentration. In addition, to increase specificity through nested PCR, we used primers internal to the predicted amplicon from the first round of PCR. Figure 4D shows the total products separated by gel

electrophoresis. Two distinct bands are visible for gene-trap-positive DNA at ~350 bp and <100 bp, while bands of corresponding size are absent for wild-type DNA. Each band size was extracted from the gel and sequenced. The ~350-bp sequence aligned to self-ligated splinkerette linker sequence.

The <100-bp fragment contained gene-trap sequence and a 24-bp sequence that did not align to the gene-trap or sequencing plasmid. This sequence included a GATC restriction site at its 3′-end, as expected from the genomic restriction digestion. Using the Ensembl BLAST program to search this sequence within the mouse genomic sequence (33), we found that the 24-bp sequence shows perfect alignment to several regions on different chromosomes, including one region in *Clock* intron 2-3 (Figure 4E). We concluded that the gene-trap inserted into *Clock* and ruled out the other genomic hits because the cDNA sequence determined earlier using the same P007F12 line showed integration of the gene-trap into *Clock* transcript. Using this alignment and the position of the GATC restriction site, we concluded that the gene-trap vector inserted between positions 77,362,594 and 77,362,595 on mouse Chromosome 5 (Figure 4E). We therefore concluded from the cDNA sequence and genomic location that we obtained a real *Clock* gene-trap allele from the P007F12 line. This allele is henceforth referred to as $Clock^{Gt}$. Furthermore, we were able to construct PCR primers to amplify the intact region of the intron in wild-type alleles (Figure 4E). Using standard PCR technique, we were thus able to identify both wild-type and gene-trap alleles to distinguish among wild-type, heterozygous and homozygous genotypes. For this reason and reasons explained later, the rest of this work concentrates on mice derived from this ES cell line.

As described in methods, ES cells from the P007F12 line were used to create chimeric mice. Backcrossing was carried out for an additional generation to the C57BL/6J strain. $Clock^{Gt}$ heterozygotes were then intercrossed. Among the progeny, we observed a Mendelian 1:2:1 genotypic ratio for the gene-trap as expected. This indicated that our PCR genotyping method was adequate and supports the genomic location determined for the gene-trap.

Vinhfield Ta
Comment:

The presence of CLOCK protein was also preliminarily tested in both wild-type and

Clock^{Gt} homozygous mice as well as in *Clock*$^{\Delta 5\text{-}6}$ homozygotes obtained from the Reppert laboratory. The *Clock*$^{\Delta 5\text{-}6}$ homozygotes were previously reported to be CLOCK-deficient by *in situ* immunocytochemical staining of the SCN and by Western analysis of whole brain and liver extracts (18). These homozygotes therefore served as a comparison for CLOCK-deficiency. Brain tissue was collected from the three genotypes, and Western blots were carried out using either the whole brain or cerebellum only. In both our gene-trap homozygotes and the *Clock*$^{\Delta 5\text{-}6}$ homozygotes, CLOCK could not be detected in the cerebellum or whole brain, while normal CLOCK expression was detected for the wild-types (data not shown; experiment and data analysis by H. Hong). This provides additional support for our use of the *Clock* gene-trap allele as a *Clock* null allele.

Functional Evidence of Clock Gene-trapping

If our gene-trap prevents CLOCK expression, we expected that complementation tests of the gene-trap allele with the wild-type and *Clock*$^{\Delta 19}$ mutant alleles could reproduce the results reported by King *et al.* (8). If the *Clock* gene-trap is fully efficient, wild-type *Clock* mRNA will not be transcribed from the *Clock*^{Gt} allele. In this case, *Clock*$^{\Delta 19}$/*Clock*^{Gt} mice would exhibit a significant ~1.5-hour period-lengthening compared to *Clock*$^{\Delta 19}$/+ mice. On the other hand, if the *Clock* gene-trap is inefficient, wild-type *Clock* mRNA expression may become evident in mice carrying the *Clock*^{Gt} allele. Depending on the efficacy of the gene-trap in this case, the phenotype of *Clock*$^{\Delta 19}$/*Clock*^{Gt} mice would result in a range of behavioral phenotypes. That is, a completely inefficient gene-trap would result in *Clock*$^{\Delta 19}$/*Clock*^{Gt} mice having periods identical to *Clock*$^{\Delta 19}$/+ mice, while moderately efficient traps would produce phenotypes intermediate between those of *Clock*$^{\Delta 19}$/+ mice and the *Clock*$^{\Delta 19}$ hemizygotes previously tested.

Therefore, in order to test gene-trap efficacy, we crossed *Clock*^{Gt} heterozygotes to *Clock*$^{\Delta 19}$ homozygotes to obtain *Clock*$^{\Delta 19}$/+ and *Clock*$^{\Delta 19}$/*Clock*^{Gt} littermates. Figure 5 shows representative activity records for both of these genotypes. Notably, of the seven *Clock*$^{\Delta 19}$/*Clock*^{Gt} mice kept in constant darkness (DD) for 10 weeks, five became arrhythmic as

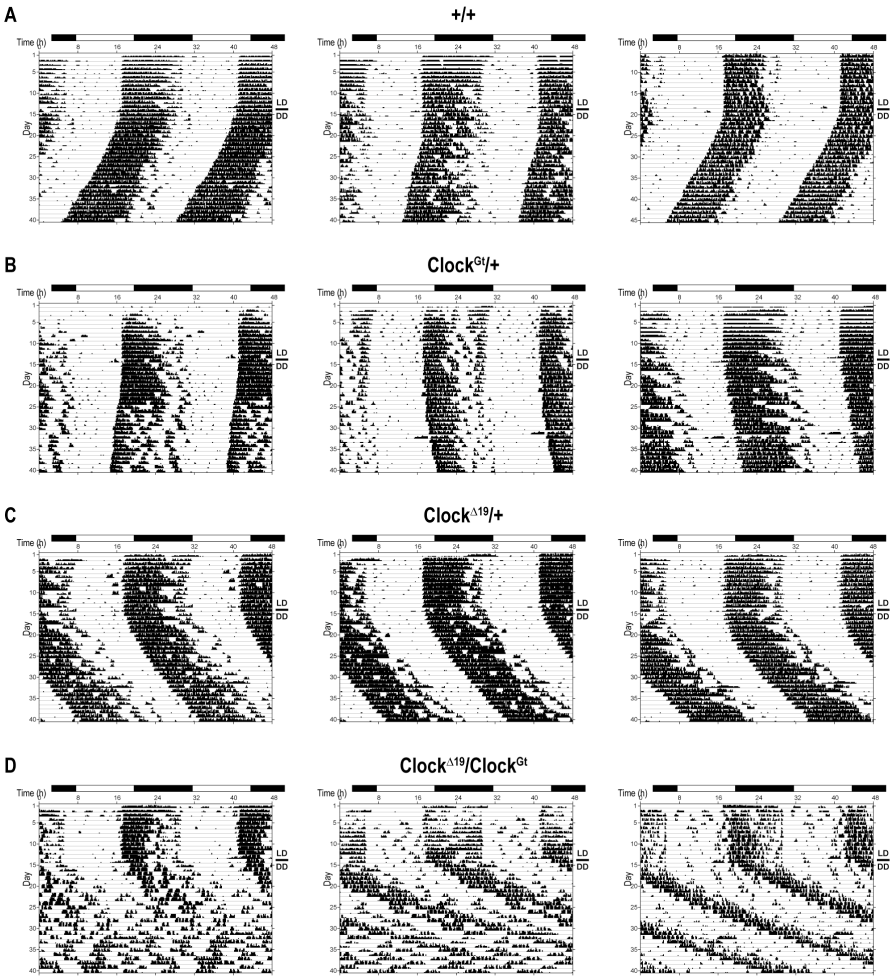

Figure 5. Representative activity records demonstrating gene-trap efficacy.
Activity is double-plotted along 48-hour periods, as in Fig. 1. All mice entrained to an LD12:12 cycle during days 1–14. The light-dark bar above each actogram indicates the light phases during entrainment (white = light, black = dark). As indicated at the right, a switch to constant darkness (DD) was made after day 14 for these mice. Wild-type (+/+; A) and *Clock*^{Gt}/+ (B) mice have noticeably shorter periods than *Clock*$^{\Delta 19}$/+ (C) and *Clock*$^{\Delta 19}$/*Clock*^{Gt} (D) mice, as can be judged by the down-rightward slope of activity onset in C and D. Some *Clock*$^{\Delta 19}$/*Clock*^{Gt} mice became arrhythmic during the second week of DD (D, left and middle), while a few remained rhythmic but exhibited very long circadian periodicity (D, right). Comparison between C and D shows that the presence of the wild-type allele (+) lessens the defect caused by the *Clock*$^{\Delta 19}$ mutant allele.

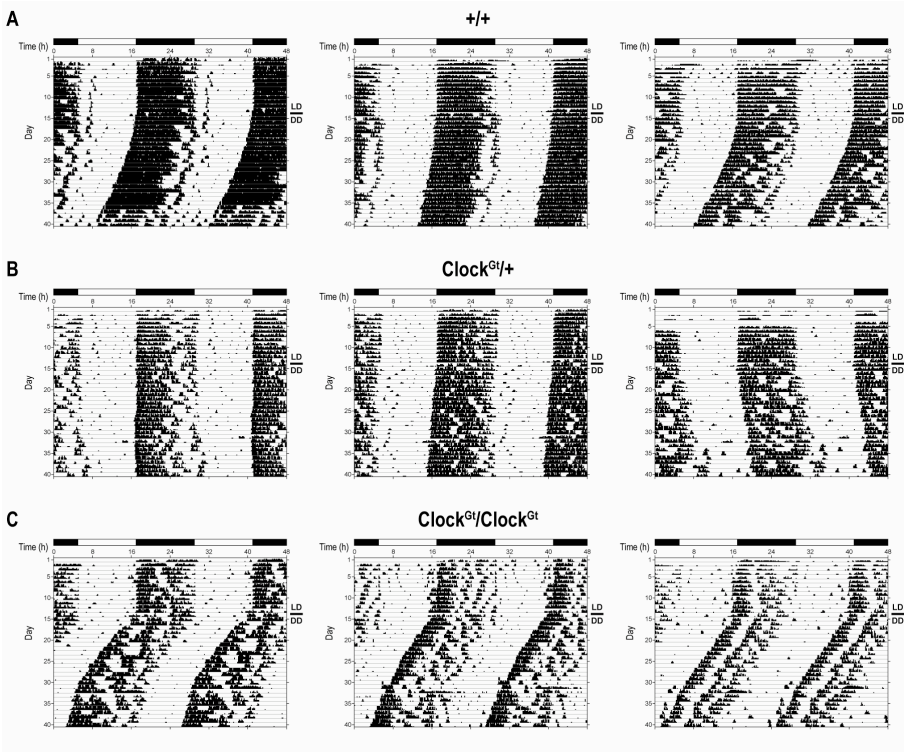

Figure 6. Representative activity records of gene-trap mice.
Activity is double-plotted along 48-hour periods, as in Figs. 1 and 5. During the first 14 days, all mice are entrained to an LD12:12 cycle indicated by the light-dark bar. Robust rhythmicity is observed for each genotype. The circadian period of $Clock^{Gt}/Clock^{Gt}$ mice (C) is short in early DD, but it lengthens noticeably by the third week. Note that the wild-type (+/+; A) and heterozygous ($Clock^{Gt}$/+) animals represented here are different from those in Fig. 5. Also note that seven of the animals represented here are littermates (excluding A, left and middle).

soon as 10 days and as late as seven weeks into DD (Figure 5D, left and middle). This disrupted circadian rhythmicity is similar to $Clock^{\Delta 19}$ homozygotes and hemizygotes previously reported (6, 8). The two mice that remained rhythmic showed very long free-running periods of ~27 and ~28 hours; one is shown on the right in Figure 5D. Rhythmic $Clock^{\Delta 19}/Clock^{Gt}$ mice displayed a free-running period (mean ± SEM) of 27.46 ± 0.37 h (n=3), which is about 2.5 hours longer than $Clock^{\Delta 19}$/+ heterozygotes whose free-running period was 24.83 ± 0.17 h (n=5) (Figure 7A).

Both of these periods were significantly longer than those of wild-type (+/+) or *Clock*^{Gt}/+ mice, whose periods are 23.56 ± 0.09 h (n=5) and 24.06 ± 0.03 h (n=22), respectively (Figure 7A).

Behavioral Circadian Rhythmicity in Constant Darkness

Based on the report by DeBruyne *et al.* (18), we expected our *Clock*^{Gt} heterozygous mice to free-run with an average period very close to that of wild-type mice. Their data also predicted that our *Clock*^{Gt} homozygous mice would have a shorter period on average. Figures 5A–B and 6A–C shows representative activity records of wild-type, heterozygous and homozygous mice. All of these mice show entrainment to the LD12:12 light-cycle during the first 14 days. After release into constant darkness, most mice show circadian periods <24 hours. Wild-type mice exhibit periods of 23.56 ± 0.09 h (n=5) in constant darkness (DD; Figure 7A). *Clock*^{Gt}/+ littermates show periods of 24.06 ± 0.03 h (n=22), which is significantly longer (ANOVA, $P<0.0001$; Tukey HSD test, $P<0.01$). On the contrary, the free-running period of *Clock*^{Gt}/*Clock*^{Gt} mice is 23.67 ± 0.07 hr (n=10), which is not significantly shorter than wild-type period (Tukey HSD test, $P>0.05$). Of the 11 *Clock*^{Gt}/*Clock*^{Gt} mice kept in DD for 9 weeks, none became arrhythmic. However, χ^2 periodogram analysis shows significant differences in the amplitude of circadian rhythmicity of *Clock*^{Gt}/+ and *Clock*^{Gt}/*Clock*^{Gt} mice compared to wild-type mice (Figure 7B). The same differences are reflected in their wheel-running activity levels (Figure 7C). Moreover, between *Clock*^{Gt}/*Clock*^{Gt} and *Clock*$^{\Delta 19}$/*Clock*^{Gt} mice, no statistical difference is found for amplitude or activity (*t*-test, $P=0.96$ and $P=0.36$, respectively).

Period measurements after prolonged time in DD yielded interesting differences among the different genotypes (Figure 8). Figure 8 shows measurements of circadian period during a 10-day interval around the second and ninth weeks of elapsed DD. For each genotype, a statistically significant change in period is observed. Period shortening is only seen in wild-type mice, while the period lengthens in both *Clock*^{Gt}/+ and *Clock*^{Gt}/*Clock*^{Gt} mice. In some *Clock*^{Gt}/*Clock*^{Gt} mice, this period-lengthening is obvious by the third week of DD (Figure 6C). The largest period difference is seen in *Clock*$^{\Delta 19}$/*Clock*^{Gt} mice, which is partly due to the

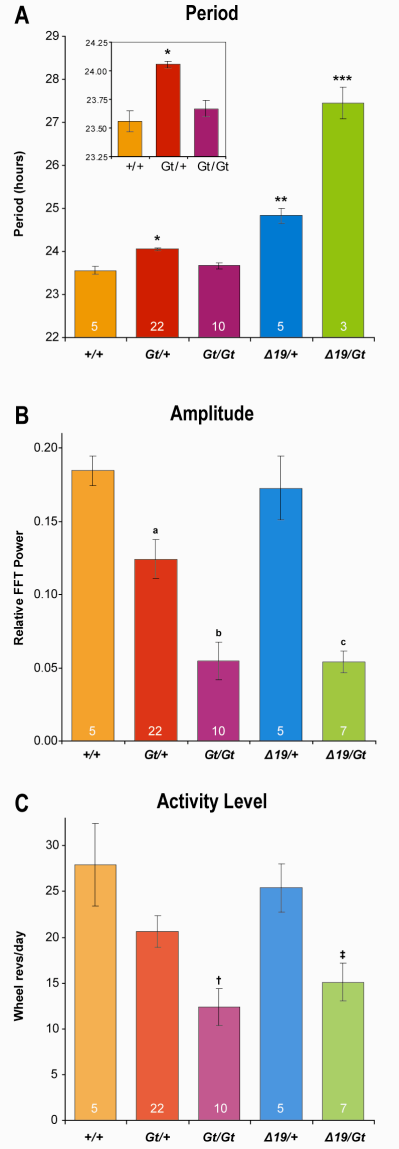

Figure 7. Circadian periodicity of mice in constant darkness.
Bar graphs show mean ± SEM. Sample number per genotype is indicated within the bars. Genotypes of mice are indicated by the alleles present: wild-type (+), gene-trap (*Gt*), and $Clock^{\Delta 19}$ (*Δ19*). (A) Free-running periods of mice are taken over the same 28-day interval in DD. Only animals rhythmic throughout this interval were counted among *Δ19*/*Gt* mice. The inset shows a magnification of the same data for three genotypes. Compared to wild-type (+/+) mice, *Gt*/+, *Δ19*/+, and *Δ19*/*Gt* mice show significantly longer periods (*t*-tests, **P*=0.003, ***P*=0.0007, ****P*<0.01, respectively). Among the gene-trap mice (left three), only *Gt*/*Gt* and wild-type mice did not differ (ANOVA; Tukey HSD, *P*>0.05). (B) Circadian amplitude is indicated by the relative FFT power from χ^2 periodogram analysis. (C) Activity level is measured by the average number of wheel revolutions per minute. Wild-type and *Δ19*/+ mice exhibit similarity of both robust amplitude and activity level (*t*-test, *P*=0.78 and *P*=0.79, respectively). In the gene-trap mice, amplitude and activity level both appear to decrease with loss of wild-type alleles. Amplitudes differ significantly from wild-type when at least one gene-trap allele is present (ANOVA, P=0.0002; Tukey HSD: *Gt*/+, ^{a}P<0.05; *Gt*/*Gt*, ^{b}P<0.01; *t*-test for *Δ19*/*Gt*, ^{c}P=0.003 compared to *Δ19*/+). Difference in activity level of *Gt*/+ is not statistically significant compared to wild-type (ANOVA, Tukey HSD, *P*>0.05), but is significant for *Gt*/*Gt* (Tukey HSD, $^{\dagger}P$<0.05). *Δ19*/*Gt* mice differ from *Δ19*/+ in activity level (*t*-test, $^{\ddagger}P$=0.015).

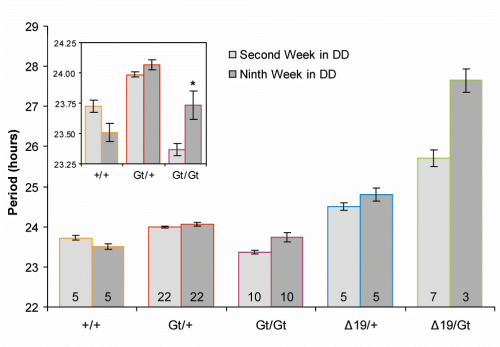

Figure 8. Changes in circadian periodicity of mice in constant darkness.
Bar graphs show the mean period ± SEM measured of a 10-day interval during constant darkness (DD). Sample number per genotype per measurement is shown within the bars. Genotypes are indicated by the alleles present: wild-type (+), gene-trap (*Gt*), and $Clock^{\Delta 19}$ (*Δ19*). The inset shows an enlargement of the same data for three genotypes. All genotypes showed statistically significant changes in period between the second week and ninth week of DD. Only wild-type period (+/+) decreases after prolonged darkness, while period lengthens for each of the other genotypes (paired *t*-tests: +/+, *P*=0.029; *Gt*/+, *P*=0.047; *Gt*/*Gt*, *P*=0.0096; *Δ19*/+, 0.028; *Δ19*/*Gt*; *P*=0.039). Of the measurements, the only period length that is not statistically different from wild-type period given the same interval in DD is the period of $Clock^{Gt}/Clock^{Gt}$ mice after prolongation in DD (*t*-test, **P*=0.12). Note that the sample number for *Δ19*/+ mice decreased because some mice became arrhythmic between the intervals measured.

averaging of only rhythmic mice, which have very long periods. Finally, it is noted that the circadian period of $Clock^{Gt}/Clock^{Gt}$ mice is initially shorter than wild-type mice by about 15 minutes (*t*-test, *P*=0.0004). After prolonged dark conditions, the increase in period of $Clock^{Gt}/Clock^{Gt}$ mice results in similar periods with wild-type (*t*-test, *P*=0.12).

Phase-Response to Light

The prior study by Vitaterna *et al.* suggested that negative alterations in wild-type *Clock* expression might have an effect on phase-resetting responses even though mice are rhythmic in DD (9). For this reason, we predicted that the light-induced response might also be affected by the lack of *Clock* expression in our gene-trap mice. We therefore characterized the behavioral phase-response by subjecting our mice to light-pulses while free-running in DD. We used 6-hour light-pulses because pulses of this duration had been reported to be more effective and

result in less variance in phase-shift magnitude in the C57BL/6J background strain (9). Furthermore, a previous study by Shimomura *et al.* showed that the time elapsed in DD before the pulse had a strong effect on the light-induced resetting-response in circadian mutant hamsters (41). Therefore, light-pulses in our experimental paradigm were initially administered after at least 3 weeks in DD, and subsequent pulses were administered at least 12 days after a prior pulse.

Figure 9 shows the activity records of several mice from our five genotypes when they are subjected to a light-pulse. Shifts in circadian phase can be seen in the actograms when the times of activity onset following a light-pulse either occur earlier or later than the times predicted by the periodicity before the light-pulse. If activity onset occurs earlier following a light-pulse, a phase-advance is observed, and the phase-shift is positive since the circadian phase is now ahead of the previous phase. If activity onset occurs later following the light-pulse, a phase-delay has occurred, and the phase-shift is negative. For each mouse, CT12 is always marked by the time of activity onset, and so, the time of the light-pulse can be determined in circadian time (CT) relative to activity onset of either the old phase or the new phase. The magnitude of phase-shifts is always determined relative to the period exhibited prior to the light-pulse by each mouse. Noticeably, the shift in circadian phase is dependent on the time of the light-pulse (Figure 9). For instance, light-pulses given during the subjective day (CT0-12), when wheel-running activity is normally low, results in little or no phase-shift. In our experiment, light-pulsing often restored wheel-running rhythmicity in arrhythmic $Clock^{\Delta 19}/Clock^{Gt}$ mice. These occurrences were also observed by Vitaterna *et al.* for arrhythmic $Clock^{\Delta 19}$ homozygotes (9). Interestingly, rhythmicity in $Clock^{\Delta 19}/Clock^{Gt}$ mice was often stable enough that the circadian phase prior to the light-pulse could be determined. As a result, phase-shifts could be measured for this genotype when pre- and post-pulse rhythms were apparent in the mouse.

Using the measured phase-shifts, we constructed phase-response and phase-transition curves for each of the five genotypes we studied (Figure 10, left and right columns, respectively). The $Clock^{Gt}/Clock^{Gt}$ (n=19), $Clock^{\Delta 19}/+$ (n=13), and $Clock^{\Delta 19}/Clock^{Gt}$ (n=18) mice clearly show

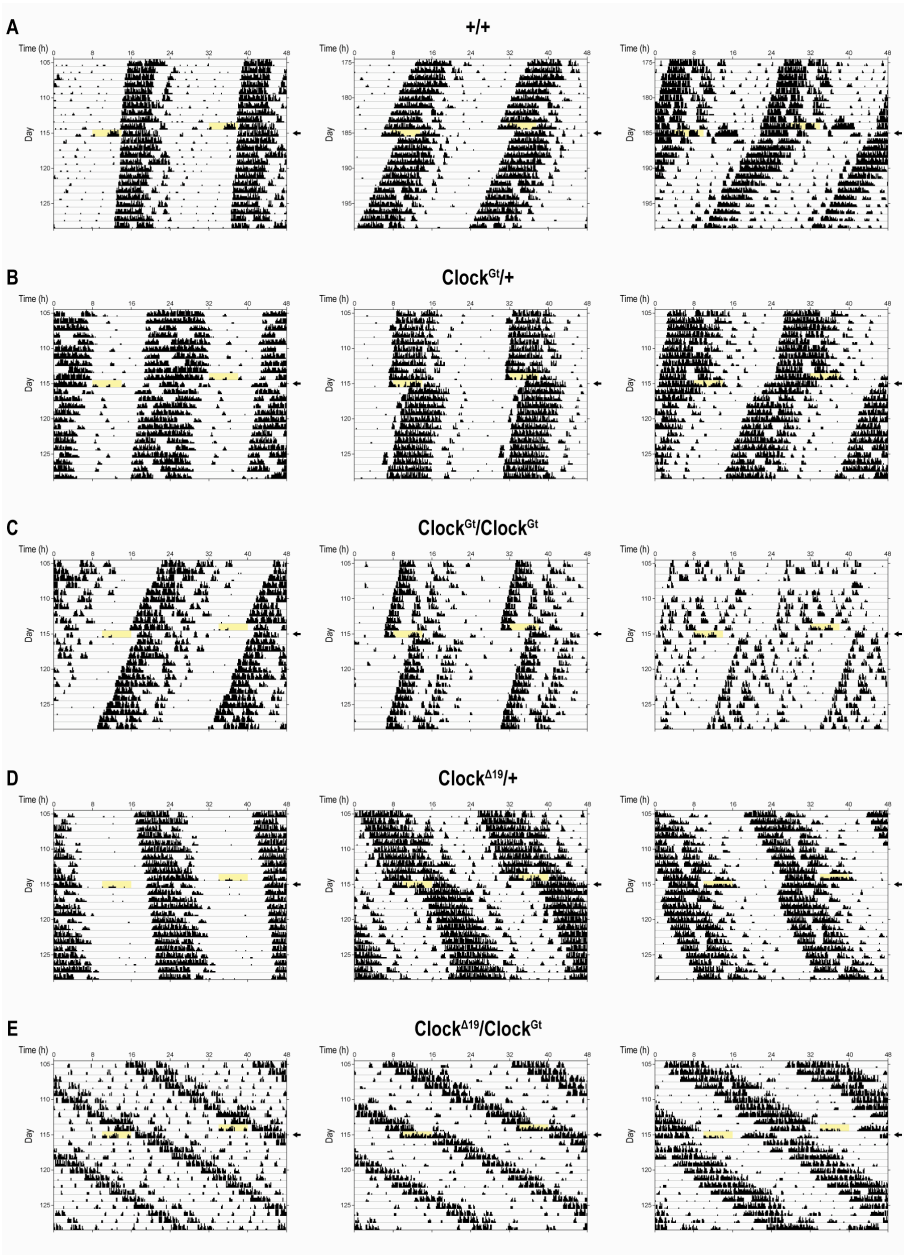

Figure 9. Representative activity records of mice subjected to a 6-hour light-pulse.
Numbers on the left indicate the day of recorded wheel-running experimentation. A light-pulse lasting 6 hours, indicated by the yellow boxes, was administered on day indicated by the arrow on the right. The light-pulse occurs during different circadian times depending on the circadian phase of the individual mouse. Note that the circadian period appears stable before and after the light pulse. Also, the *Clock*$^{\Delta 19}$/*Clock*^{Gt} mice (E) shown here are rhythmic before and after they receive the pulse, permitting their phase-shifts to be measured.

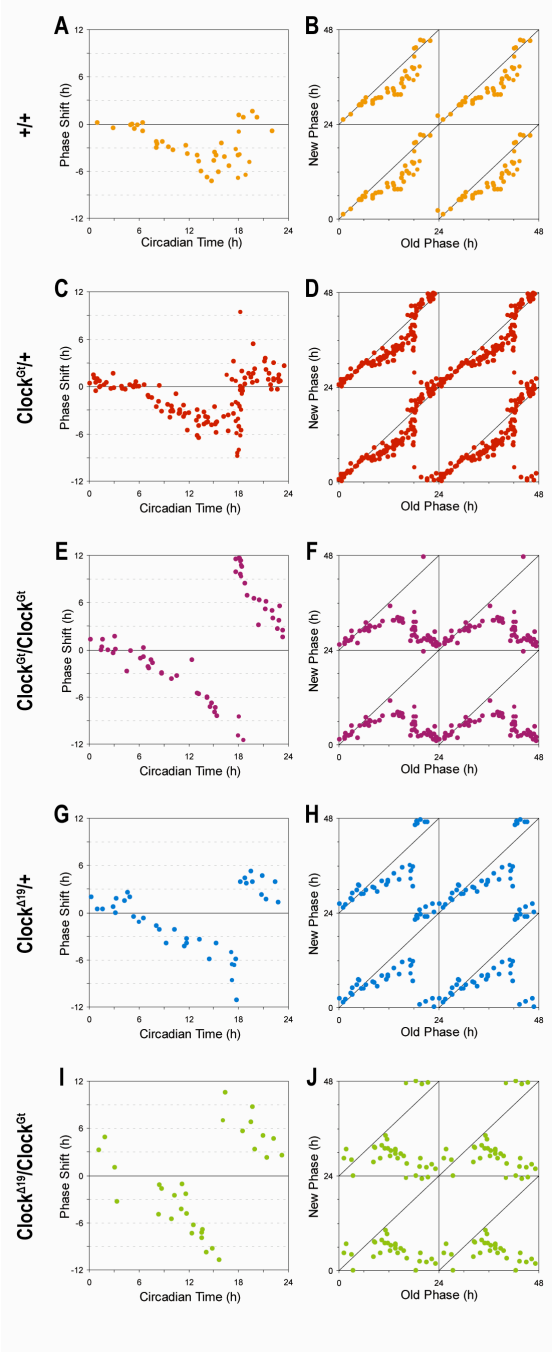

Figure 10. Behavioral phase-response and phase-transition curves. These phase-resetting curves are constructed using measurements of behavioral phase-shift in response to 6-hour light pulses. (A, C, E, G and I) Phase-response curves are shown for wild-type (+/+; n=14; A), *Clock*^{Gt}/+ (n=19; C), *Clock*^{Gt}/*Clock*^{Gt} (n=20; E), *Clock*$^{\Delta 19}$/+ (n=13; G), and *Clock*$^{\Delta 19}$/*Clock*^{Gt} (n=18; I) mice. The abscissa indicates the circadian time (CT) at the beginning of the light-pulse. The ordinate indicates the phase-shift due to the light-pulse given at that CT. Phase-delays are negative, and phase-advances are positive. (B, D, F, H and J) Corresponding phase-transition curves are shown for each genotype. The abscissa indicates the CT when the pulse was given relative to the old phase. The ordinate indicates the CT of the pulse relative to the phase of the circadian rhythm after the light-pulse. Both axes are double-plotted. Points falling along the diagonal line (slope=1) represent no change in phase, indicating Type 1 responses. Points falling onto a horizontal (slope=0) indicate Type 0 responses.

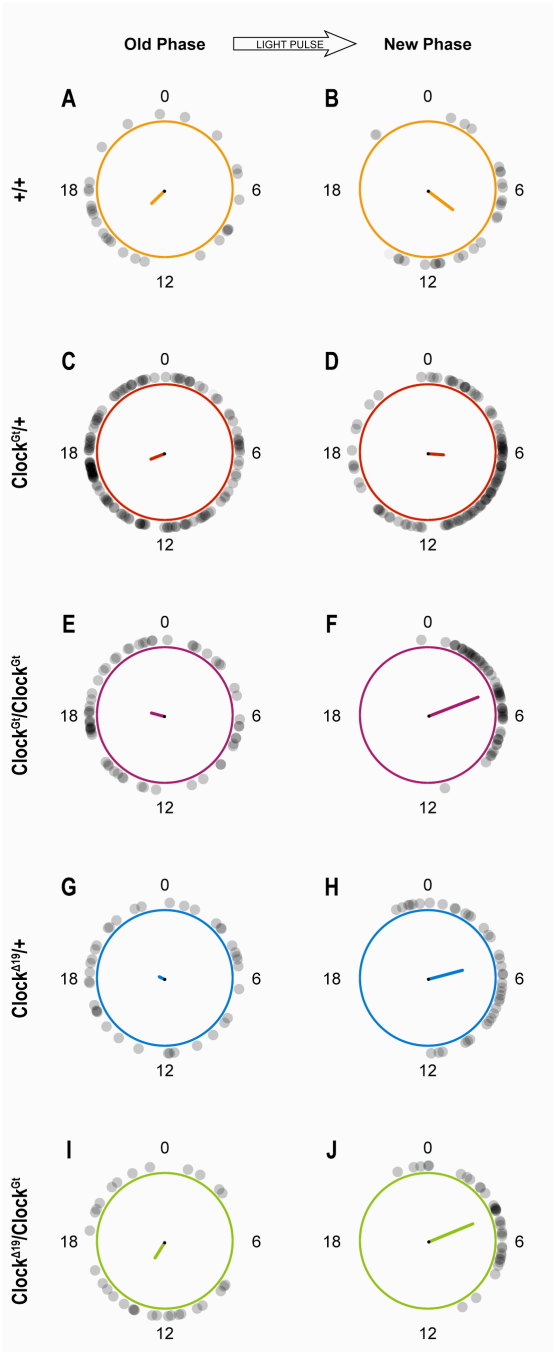

Figure 11. Rayleigh plots comparing initial and reinitiated phases in response to light-pulsing.

Points on the Rayleigh plot indicate the phase of the circadian cycle when a light-pulse was administered, either relative to the rhythm before the pulse ("old phase," left column) or relative to the new rhythm after the pulse ("new phase," right column). Isochrons of four circadian times (CTs) are labeled on the outside of the circle. In these plots, all data points are gray. Overlap causes darkening to permit visualization of density. Vectors in the middle of the circle point in the direction of the (circular) mean phase, and vector magnitude is a measure of the strength of concentration about the mean phase. For a random, uniform distribution, the vector is a zero vector. (A, C, E, G, I) Old phases are more scattered throughout the circadian cycle because light-pulses were administered at random times. Clustering of light-pulse times is only significant for $Clock^{Gt}/+$, meaning that the time of light-pulse administration was not completely random (Rayleigh test, $P<0.05$; C). For all genotypes, the reinitiated phases do cluster according to statistical analysis (Rayleigh test, $P<0.05$). However, the strength of clustering is weaker for +/+ (B) and $Clock^{Gt}/+$ (D) as indicated by the shorter vector length. For $Clock^{Gt}/Clock^{Gt}$ (F), $Clock^{\Delta 19}/+$ (H), and $Clock^{\Delta 19}/Clock^{Gt}$ (J) mice, new phases cluster strongly around CT4.5-5.0.

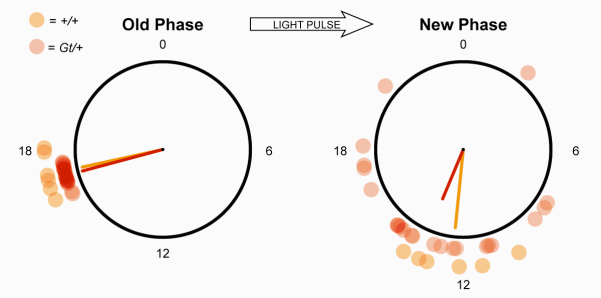

Figure 12. Phase dispersion due to light-pulsing at CT17.
Rayleigh plots are drawn for the old phase and new phase for both wild-type (+/+) and *Clock*^{Gt}/+ (*Gt*/+) mice. All data points are the same shade of red or orange, and overlap causes darkening. Mean vectors point to the circular mean of the data of corresponding color. Data points reflect light-pulses administered at CT16-18. (Left) The mean vectors point toward CT17, indicating the mean time when the light-pulses were administered. The vector magnitudes indicate strong concentration of the light-pulses at CT17. (Right) After the light-pulse, wild-type phases are still strongly concentrated with low deviation about the mean (s=1.3 h). *Clock*^{Gt}/+ mice still show statistically significant concentration (Rayleigh test, P<0.05) but also wider deviation (s=3.2 h) than wild-type.

Type 0 phase-resetting response patterns with the breakpoint occurring at CT17–18 (*cf.* Figure 3). On the other hand, wild-type (n=14) and *Clock*^{Gt}/+ (n=19) mice exhibit the weaker Type 1 response pattern. The phase curves for wild-type and *Clock*$^{\Delta 19}$/+ mice closely resemble those determined by Vitaterna *et al.* (9). The phase-response curve for the *Clock*^{Gt}/*Clock*^{Gt} mice also shows ~7-hour phase-advances for pulses given at CT20. This agrees with the strong phase-advances observed at ZT20 by DeBruyne *et al.* (18).

Visual comparison between wild-type and *Clock*^{Gt}/+ mice suggests that there are some subtle differences in their behavioral phase-resetting responses. For both genotypes, the phase-delay region (approximately CT12–17) is larger relative to the phase-advance region (approximately CT17–24). The maximum phase-delay observed for nearly all of the light-pulses was 7 hours for both genotypes. However, several *Clock*^{Gt}/+ mice exhibited phase-delays of up to 9 hours. Moreover, the phase-advance region appears to be increased in *Clock*^{Gt}/+ mice compared to wild-type mice, with a maximum phase-advance of about 4 hours compared to 2 hours in wild-type mice. Further comparison between wild-type and *Clock*^{Gt}/*Clock*^{Gt} mice shows

no difference of the phase-resetting response during the subjective day (CT0–12; Figures 10A and 10E). However, we noticed that the $Clock^{Gt}/Clock^{Gt}$ mice appear to show stronger magnitudes of light-resetting responses during the subjective night (CT12–24) than $Clock^{\Delta 19}/+$ mutants. This enhanced behavioral phase-resetting response is reflected in the larger phase-delay and phase-advance values observed for $Clock^{Gt}/Clock^{Gt}$ mice compared to those for $Clock^{\Delta 19}/+$ mice (Figures 10E and 10G).

To compare differences in the strength of resetting, Rayleigh plots were constructed using the circadian phase both prior to and following the pulse (Figure 11). No clustering is expected for circadian time (CT) prior to the pulse because the old phase merely indicates when random light-pulses were administered (Figured 11, left column). However, statistically significant clustering of the old phase is seen for $Clock^{Gt}/+$ mice, meaning light-pulses were not administered uniformly throughout the circadian cycle (Rayleigh test, $P<0.05$). For the weak Type 1 resetting-responses, the reinitiated phases, or new phases, are not expected to cluster significantly because the position of the old phase is only weakly pushed towards a new phase by the light-pulse. In contrast, the strong Type 0 resetting-response results in significant clustering of the new phases at a particular CT. This strong clustering is indeed observed for $Clock^{Gt}/Clock^{Gt}$, $Clock^{\Delta 19}/+$, and $Clock^{\Delta 19}/Clock^{Gt}$ mice. Their old phases are not concentrated (Rayleigh test, $P>0.05$; Figures 11E, 11G and 11I), but following the light-pulse, significant clustering (Rayleigh test, $P<0.05$) is seen at CT4.6 for $Clock^{Gt}/Clock^{Gt}$ and $Clock^{\Delta 19}/Clock^{Gt}$ mice or CT5.0 for $Clock^{\Delta 19}/+$ mice. While the new phases are similar (parametric tests, $P>0.05$), the new phase of $Clock^{Gt}/Clock^{Gt}$ mice shows less angular deviation about the mean (mean angular deviation, $s=0.28$ h) compared to $Clock^{\Delta 19}/+$ and $Clock^{\Delta 19}/Clock^{Gt}$ mice ($s=0.58$ h and $s=0.44$ h, respectively).

The data collected also show significant clustering of new phases for wild-type and $Clock^{Gt}/+$ mice (Figure 11B and 11D). For the $Clock^{Gt}/+$ mice, this can be explained by concentration of light-pulse onsets at CT16.5. On the other hand, clustering for wild-type mice is probably due to both clustering of light-pulse onset and low sample number. This explains the

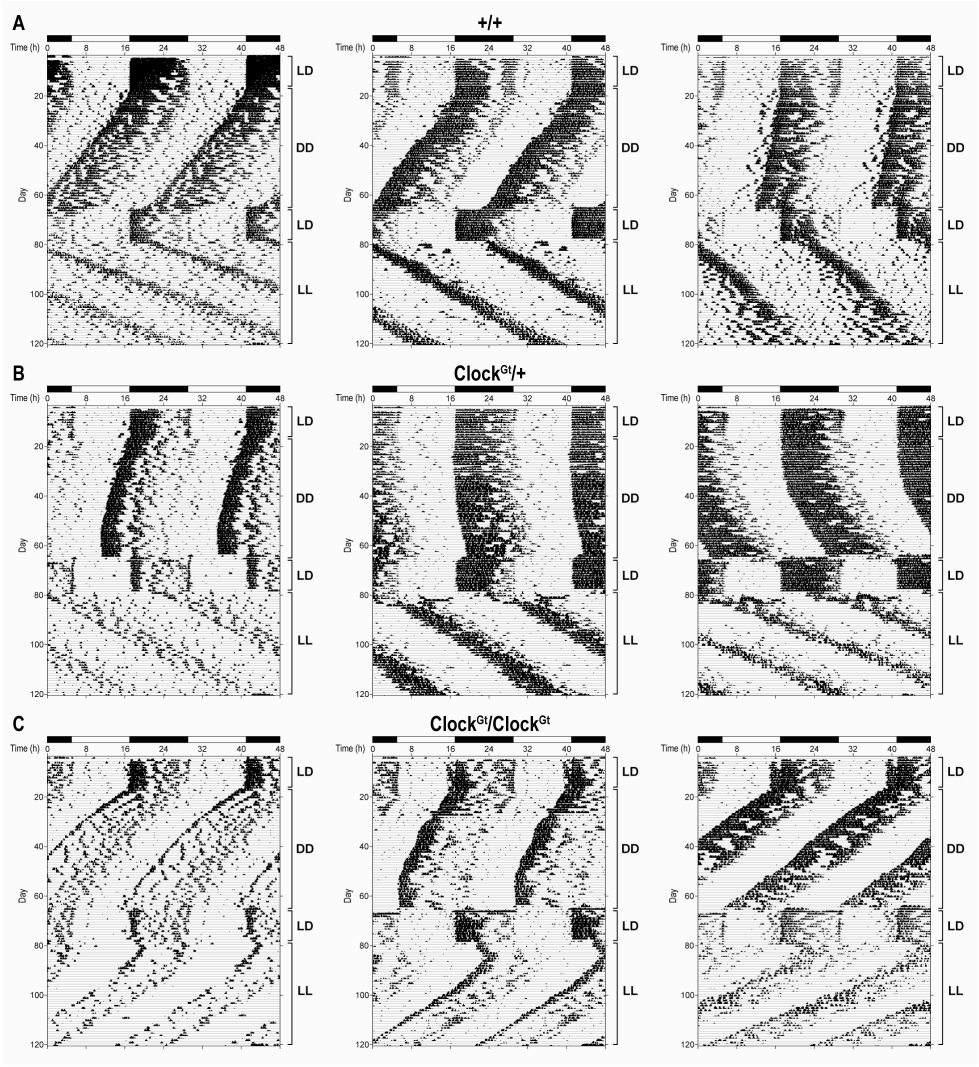

Figure 13. Representative activity records of mice in constant light.
Mice were first entrained to an LD12:12 cycle (LD) and then released into constant darkness (DD). Subsequently, the mice were re-entrained to LD and then subjected to constant light (LL) conditions. Light conditions are indicated on the right of each actogram. The bar on top indicates the phases of the LD cycle (white = light; black = dark). *Clock*^{Gt}/*Clock*^{Gt} mice (C) have short, <24-hour periods in LL compared to wild-type (+/+; A) or *Clock*^{Gt}/+ (B) mice, which have long, >24-hour periods.

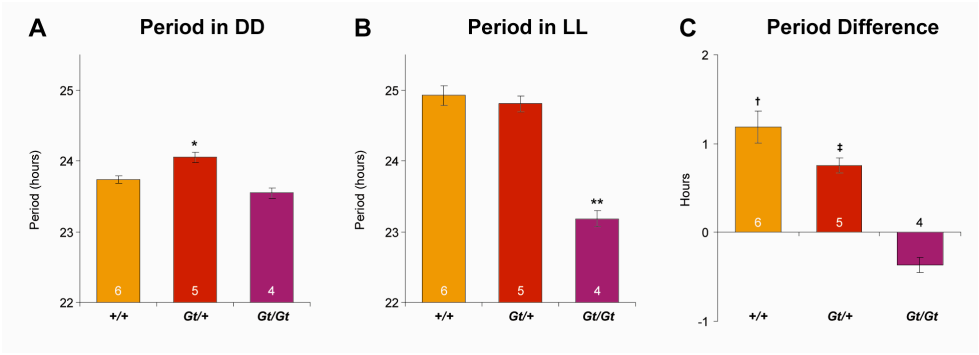

Figure 14. Comparison of circadian period in constant light conditions.
Fifteen mice were subject to both constant dark (DD) and constant light (LL) conditions. Period measurements are taken using 28 days of activity. Bar graphs represent mean ± SEM. Sample number per genotype is indicated within the bars. (A) In DD, *Clock*^{Gt}/+ mice (*Gt*/+) have a significantly longer period (+/+) (ANOVA, P=0.002). The periods of *Clock*^{Gt}/*Clock*^{Gt} (*Gt*/*Gt*) and wild-type mice are not statistically different (*t*-test, P=0.21). (B) In LL, +/+ and *Clock*^{Gt}/+ mice have long periods (mean±SEM) of 24.92±0.14 h and 24.81±0.11 h, respectively. This difference is statistically insignificant (*t*-test, P=0.54). In contrast, *Clock*^{Gt}/*Clock*^{Gt} mice have a significantly shorter period, 23.18±0.11 h, compared to wild-type or *Clock*^{Gt}/+ mice (ANOVA, $^{**}P<0.00001$). (C) The time difference between periods in DD and LL is compared per genotype. Wild-type and *Clock*^{Gt}/+ mice have significantly longer periods in LL (paired *t*-tests, $^{\dagger}P$=0.001 and $^{\ddagger}P$=0.0008, respectively). The shorter period seen in *Clock*^{Gt}/*Clock*^{Gt} mice is statistically insignificant (paired *t*-test, P=0.14).

apparent discrepancy with data obtained by Vitaterna *et al.*, which does not show significant clustering of new phases (9).

Rayleigh plots were also used to compare the effect of light-pulsing for the Type 1 responsive mice (Figure 12). Data points showing that light-pulses were given between CT16 and CT18 were isolated and plotted. Interestingly, while the old phases are concentrated at CT17, *Clock*^{Gt}/+ mice show greater dispersion of new phases following the light-pulse than wild-type mice (s=3.2 h compared to s=1.3 h).

Behavioral Circadian Rhythmicity in Constant Light

Since *Clock*^{Gt}/*Clock*^{Gt} mice showed enhanced responses to light, we also tested our gene-trap mice in constant light (LL) conditions. Previous experiments show that mice of the C57BL/6J background strain have long periods, *i.e.* >24 hours, in LL. This includes wild-type

mice and $Clock^{\Delta 19}$/+ mutants (unpublished data). As shown in Figure 13 (experiment by J. L. Chong), our gene-trap mice entrain normally and exhibit short free-running periods in DD as expected from our previous experiment (*cf.* Figure 6; and Figure 13). The mice were then re-entrained to LD12:12 for 14 days and subsequently kept in constant light. $Clock^{Gt}/Clock^{Gt}$ mice show long periods in LL for the initial 3–13 days. After this, the circadian period rapidly becomes short, *i.e.* <24 hours. As measured during a steady 28-day interval in LL, their circadian period (mean ± SEM) is 23.18 ± 0.11 h (n=4) (Figure 14). This period is significantly shorter (ANOVA, $P<0.00001$; Tukey HSD, $P<0.01$) than both wild-type period (24.92 ± 0.14 h; n=6) and heterozygote period (24.81 ± 0.11 h; n=5). In contrast, $Clock^{Gt}$/+ mice in LL are indistinguishable from wild-type (Tukey HSD, $P>0.05$). When the same mice are compared between DD and LL, only $Clock^{Gt}/Clock^{Gt}$ mice do not show significantly different periods between the two conditions (paired *t*-test, $P=0.14$; n=4).

Discussion

Molecular and functional comparisons of the *Clock* gene-trap mice to mice studied previously have been important toward identifying CLOCK-deficiency in our mice. Western analysis shows that CLOCK protein is undetectable in the brain of $Clock^{Gt}/Clock^{Gt}$ mice, similarly to that of the CLOCK-deficient mice studied by DeBruyne *et al.* (18). Behaviorally, we were able to reproduce allelomorph analysis of the $Clock^{\Delta 19}$ mutant allele using our gene-trap allele in place of the chromosomal deletion used by King *et al.* (8). In their study, the deletion of one *Clock* allele in combination with the $Clock^{\Delta 19}$ mutant allele causes a behavioral phenotype that is more severe than that of mice which express both the wild-type and $Clock^{\Delta 19}$ mutant alleles. In concordance with these previous results, we observed that $Clock^{\Delta 19}/Clock^{Gt}$ mice have a drastically lengthened circadian period (~2.5 hours) compared to that of $Clock^{\Delta 19}$/+ littermates. This heightened defect in $Clock^{\Delta 19}/Clock^{Gt}$ mice therefore suggests that wild-type CLOCK protein expression is not present to abate the period-lengthening effect of mutant $CLOCK^{\Delta 19}$. Further support for CLOCK-deficiency comes from the observed arrhythmicity of some of these

heterozygotes, which is similar to $Clock^{\Delta 19}/Clock^{\Delta 19}$ mice. This observation suggests a more severe defect than those shown in the *Clock* deletion strains from the previous study. This difference may be due to strain differences, especially because mice used in the original analysis were mixed with the C3HeB/FeJ background, which may have contained a suppressor of the *Clock* mutation that is found in those inbred strains (unpublished data). Additionally, mice from this previous study were kept in DD for only about 3 weeks. This may have been an insufficient amount of time for arrhythmic wheel-running behavior to surface, since 4 weeks in DD elapsed before some of our $Clock^{\Delta 19}/Clock^{Gt}$ mice became arrhythmic.

Both the molecular and behavioral assays from the current experimental data strongly point to the successful use of gene-trap mutagenesis to generate a null allele of a wild-type, mammalian circadian gene. Of course, the caveat is that gene-trapping still requires extensive follow-up experiments to test its efficacy. This is clearly demonstrated by our identification of the W174F05 line as a false-positive for vector insertion of the gene-trap into the *Clock* gene. For the P007F12 line, the splice junction between *Clock* and the gene-trap was successfully identified by RT-PCR and cDNA sequencing. Along with β-gal staining, these experiments suggest efficacy of the gene-trap in the P007F12 line. Meanwhile, the integrative junction between the retroviral insert and *Clock* intron was identified by splinkerette PCR and DNA sequencing. Although the length of the genomic sequence recovered by this method was only 24-bp, the cDNA sequence eliminated the possibility that the gene-trap had integrated outside of *Clock* intron 2-3, and the 24-bp sequence pointed to integration into the intron.

While molecular efficacy of the gene-trap has been shown in mouse ES cells and CLOCK-deficiency suggested in the *in vivo* brain, additional conclusive evidence that the gene-trap creates a *Clock* null allele is appropriate. Efficacy is not guaranteed by integration of the gene-trap into just some of the spliced transcript, since it is possible that inefficient transcriptional termination at the gene-trap and inefficient splicing of the gene-trap into mRNA transcript could result in expression of untrapped, functional wild-type transcript. In this way, alternative splicing of *Clock* transcript might result from tissue-specificity, such that gene-

trapping does not produce a whole-animal, *Clock* null mutant. To further show functioning of the gene-trap in tissues, β-gal staining of tissue extracts might be used to show expression of *β-Geo* and Northern analysis to show the absence of downstream *Clock* exons. More evidence for CLOCK-deficiency should also come from *in situ* hybridizations of mouse brain sections because this method is most spatially and quantitatively sensitive to *Clock* expression. In particular, the specific region of the suprachiasmatic nuclei (SCN) must be examined since the SCN plays the central role in mammalian circadian timing. Additional Western analysis using peripheral tissues such as lung and liver, which are known to express the core circadian genes (1, 2, 23), might also be completed to emphasize the absence of *Clock* gene expression in peripheral tissues.

Behavioral analysis of our *Clock* null mutant mice, the $Clock^{Gt}$ homozygotes, provides interesting information about the core circadian oscillator. Even though *Clock* expression is absent, behavioral circadian rhythmicity is still evident in constant darkness (DD), so far as behavior is indicated by wheel-running activity. This result agrees with data from the $Clock^{\Delta 5\text{-}6}$ mutants reported by DeBruyne *et al.* (18). In contrast to these *Clock* null mice, null mutants of the partner of *Clock*, *Bmal1*, are completely arrhythmic in DD (44). This might suggest that *Clock* is not a necessary gene for rhythmic wheel-running behavior. Or, this can also suggest that a gene other than *Clock* compensates for the absence of *Clock* expression. In this case, *Clock* and the compensating gene would have complementary roles in controlling rhythmic wheel-running behavior. Null mutations to both *Clock* and the compensating gene might then show arrhythmicity. This pattern would be similar to the relationship between *mPer1* or *mPer2*, where single-gene *mPer1* null mutations lead to mild circadian defects while double-gene null mutations abolish rhythmicity (12, 13) Very recently, Debruyne *et al.* have demonstrated this idea, showing that double-gene null mutations to *Clock* and *Npas2*, a paralog of *Clock*, lead to complete arrhythmicity in DD (45-47). Their data therefore suggests that *Npas2* can compensate for *Clock* function in the *Clock* null mutant, and that these paralogs have at least partially overlapping contributions to circadian oscillation in the SCN.

Despite our finding that CLOCK-deficiency does not cause a dramatic effect on the free-running period of mice, the circadian rhythmicity of the *Clock* null mice is not identical to that of wild-type. First, the free-running period of $Clock^{Gt}$ homozygotes is shorter only in early DD compared to wild-type. This difference of about 15 minutes agrees with the study by DeBruyne *et al.* (18). However, the period of $Clock^{Gt}$ homozygotes also lengthens by about 20 minutes over the course of eight weeks in DD. Lengthening occurs for $Clock^{Gt}$ heterozygotes, as well, but to a lesser extent. This change was probably not observed previously because mice were only kept in DD for four weeks in their experiment (18). Changes in period over time in DD provide interesting information. Because the period of $Clock^{Gt}$ homozygotes was observed to lengthen quickly about three weeks into DD, entrainment to the light-dark cycle may have a residual effect on the free-running period in early DD. Elapsed period-lengthening is suggestive of defectiveness in the circadian rhythmicity, as wild-type mice show the opposite trend of period-shortening in DD. Further suggesting circadian defectiveness are reductions in the circadian amplitude and activity levels of $Clock^{Gt}$ mice, which seem to correlate with the loss of expression of the wild-type allele by either the wild-type mouse (+/+) or $Clock^{\Delta 19}$/+ mutant. Importantly, these results differ from those obtained by DeBruyne *et al.*, who found that only activity level and not amplitude was significantly decreased in *Clock* null mutants (18, 45). Some of this difference may be attributed to background strain differences since the gene-trap mice come from slightly different genetic backgrounds from previous studies.

Surprisingly, $Clock^{Gt}$ heterozygotes show a 30-minute longer period compared to wild-type mice in DD. This is perplexing considering that $Clock^{Gt}$ homozygotes show the shortening compared to wild-type mice. Based on the circadian amplitude and activity of $Clock^{Gt}$ heterozygotes, which is intermediate between those of wild-type and $Clock^{Gt}$ homozygous mice, one might suggest that the $Clock^{Gt}$ heterozygotes exhibit haploinsufficiency. One might further speculate that only the complete loss of *Clock* gene expression triggers a compensatory mechanism that results in the shortened period observed in $Clock^{Gt}$ homozygotes. To address this issue, further experimental studies may make use of real-time conditional expression

systems, such as the tetracycline transactivator system that has been created in the Takahashi laboratory to control spatial and temporal expression of *Clock* (48).

The enhanced light-induced phase-resetting response observed in *Clock* null mutants provides strong evidence that the core circadian oscillator is altered by reduced CLOCK function. The absence of *Clock* expression results in strong, Type 0 responses, while the presence of just one copy of the wild-type allele is sufficient to produce a Type 1 response. The phase-resetting effect caused by CLOCK-deficiency closely resembles that caused by the $Clock^{\Delta 19}$ mutation, since these mice all showed re-initiation of the circadian phase toward CT5 after each light-pulse. Our finding shows discrepancies in the data reported by DeBruyne *et al.* (18). Contrary to their evidence that phase-delaying is deficient in *Clock* null mutants, we clearly show enhancement of circadian responses to light in general, which includes phase-delaying in the early subjective night. This as well as our evidence for a residual effect of LD entrainment suggests that their experimental paradigm was insufficient to properly address light-induced resetting responses.

While sample number was considerably low for wild-type mice, enough data was gathered for comparison of the wild-type phase-response and phase-transition curves to those determined by Vitaterna *et al.* (9). Both experiments show similar responses for wild-type mice, even though mice in the present study were initially kept for much more than three weeks in DD prior to their first light-pulse. Comparisons of data collected from the first light pulse and subsequent ones show a lack of correlation between the length of time the mice spend in DD and the magnitude of their light response (data not shown). Therefore, the light-induced resetting-response does not alter with elapsed time in DD in wild-type mice. In addition, the shapes of the phase-response and phase-transition curves (Type 1) do not differ considerably between wild-type and $Clock^{Gt}$ heterozygous mice. However, examination of pulses given at CT17 reveals that the new phases disperse more widely in $Clock^{Gt}$ heterozygous mice compared to wild-type mice. Comparison at CT17 is important because this is when the breakpoint in the phase-response curve occurs for $Clock^{Gt}$ homozygotes, and the difference between Type 0 and Type 1 responses

is most distinct at the breakpoint. For the weak Type 1 response, phase-shifts from this circadian phase are small because the phase-resetting stimulus is too weak to push the phase of circadian oscillation past what is called the singularity point in the limit-cycle model. Conversely, for strong Type 0 responses, phase-shifts from CT17 are large because the phase-resetting stimulus pushes the oscillation to a new phase past the singularity point. Intermediate between Type 0 and Type 1, the stimulus pushes the oscillation very close to the singularity point, resulting in a wider dispersion of the new phase. Therefore, the wider dispersion suggests that the resetting-responses in $Clock^{Gt}$ heterozygous mice are somewhat intermediate between the responses of wild-type and *Clock* null mice, though it is still a Type 1 response. This case suggests that $Clock^{Gt}$ heterozygous mice are subtly affected by the loss of one wild-type *Clock* allele.

It should be noted that data presented in the Rayleigh plots can be inconclusive about the type of resetting-response. This is because data for the new phase are easily biased by the time of the light-pulse onset. This is probably the reason that statistically significant clustering of the new phase is observed for $Clock^{Gt}$ heterozygotes, even though they show Type 1 responses. Because light-pulses for these mice were significantly concentrated at CT16, and pulses given at this time normally cause resetting to about CT10, new phases were also concentrated. While statistically significant clustering was not observed in the old phases of wild-type mice, partial concentration and lower sample number contribute to the observed concentration of their new phases at CT8. Indeed, Vitaterna *et al.* did not find significant clustering of new phases for wild-type mice (9). Nevertheless, Rayleigh plots for Type 0 responsive mice clearly indicated clustering of new phases by the way all new phases fell within an approximately 12-hour interval.

The altered responses to light in *Clock* null mice are further distinguished by their behavior in constant light conditions (LL). In contrast to the long periods seen in $Clock^{\Delta 19}$/+, $Clock^{\Delta 19}$/ $Clock^{\Delta 19}$, and wild-type mice in LL, $Clock^{Gt}$ homozygotes have a drastically shortened period of 23.2 hours. Because mice are constantly receiving stimulus to shift their phases in constant light, there is a cumulative effect of light that is determined by their phase-response

curves. In *Clock* null mice, the magnitude of phase-shifts that occur in the phase-advance region (~CT17-24) are much larger than that of $Clock^{\Delta 19}$/+ and wild-type mice. This suggests that the short period of *Clock* null mice in LL may be a result of the phase-advancing region having a larger cumulative effect on circadian behavior than the phase-delaying region. So, although the phase-response curves suggest that the light response of $Clock^{\Delta 19}$ mutants and *Clock* null mutants are the same (Type 0), behavioral differences become apparent in constant light conditions. These results show that the $Clock^{\Delta 19}$ mutation and null *Clock* expression have significantly different effects on light-induced resetting-responses.

The difference in circadian amplitude suggests that the enhanced light-induced phase-response in *Clock* null mice might be due to decreased amplitude of molecular oscillations. This is the explanation given for enhanced responses in $Clock^{\Delta 19}$ heterozygotes (9), even though heterozygotes show robust circadian rhythms. This contrast adds to the suggestion that the enhanced light responses between $Clock^{\Delta 19}$ and $Clock^{Gt}$ mice have different underlying mechanisms. In the present experiment, decreased circadian robustness also correlates with enhanced responses in $Clock^{\Delta 19}$/$Clock^{Gt}$ heterozygotes and with intermediate responses in $Clock^{Gt}$ heterozygotes. However, this data is only suggestive, and a molecular mechanism would have to be investigated to better explain the enhanced resetting-response in *Clock* null mice. This will involve time-course experiments in which tissue samples are extracted from mice at different circadian times and assayed for expression of the core circadian genes. Although DeBruyne *et al.* shows this sort of time-course data for mRNA and protein levels, tissue in their experiment are collected during the first day in DD after LD entrainment (18). Since it has been shown that LD entrainment has a residual effect on circadian gene expression in the SCN during early DD (41, 9), it will be more appropriate to assay gene expression at least three weeks into DD. In addition to the time-course experiment, induction of gene expression by light in the SCN should also be determined to evaluate the responsiveness of the core circadian oscillator to light input signals. In particular, expression analysis and topographic expression of the two core circadian genes that are rapidly induced by light, *mPer1* and *mPer2* in the SCN (28), may

provide invaluable data that would allow us to correlate temporal and spatial gene expression with the observed behavioral phenotypes.

In this study, we have demonstrated the importance of the *Clock* gene in determining the magnitude of light-induced resetting responses. While the *Clock* gene is not necessary for the maintenance of circadian wheel-running behavior in constant darkness, weakness of the circadian amplitude in its absence points to it having a crucial role in amplifying the robustness of behavioral oscillations. Furthermore, the enhanced light resetting-responses show that *Clock* expression is necessary for normal processing of light-input signals within the core oscillator. It would be interesting to see whether *Npas2* null mutants and double null mutants of *Clock* and *Npas2* exhibit similar resetting-responses as *Clock* null mice. Future behavioral characterization and expression analysis of circadian genes in the SCN of these mutants would yield novel insights into the mechanisms that are vital for light entrainment.

Acknowledgments

I would like to thank Jason L. Chong for the phenomenal support, training, and guidance toward taking up and completing this project. Thanks also to Joseph S. Takahashi for providing space and funds to work in his laboratory. This project was made possible in part by summer research grants awarded by the Weinberg College of Arts and Sciences and the Undergraduate Research Grant Committee at Northwestern University. I also acknowledge my colleagues for their help: Hee-kyung Hong and Amira Jyawook for training in animal facilities; Caroline H. Ko for help with Lac-Z staining of cell cultures; Hee-kyung Hong for Western analysis of protein expression in brain extracts; Weimin Song for *in vitro* injection of ES cells; Amanda Falk for technical assistance with DNA sequencing; and Martha H. Vitaterna for information on the Rayleigh plots.

References

1 Reppert SM, Weaver DR. (2002) Coordination of circadian timing in mammals. *Nature* **418**:935-941.

2 Lowrey PL, Takahashi JS. (2004) Mammailian Circadian Biology: Elucidating Genome-Wide Levels of Temporal Organization. *Annu. Rev. Genomics Hum. Genet.* **5**:407-41.

3 Dunlap Jay C., Jennifer J Loros, and Patricia J Decoursey, eds. *Chronobiology: Biological Timekeeping*. Sunderland: Sinaur Associates, 2004. pp26-105.

4 Harmer SL, Panda S, Kay SA. (2001) Molecular bases of circadian rhythms. *Annu. Rev. Cell Dev. Biol.* **17**:215-53.

5 Matsuo T, Yamaguchi S, Mitsui S, Emi A, Shimoda F, Okamura H. (2003) Control mechanism of the circadian clock for timing of cell division in vivo. *Science* **302**:255-59.

6 Vitaterna MH, King DP, Chang AM, Kornhauser Jm, Lowrey PL, McDonald JD, Dove WF, Pinto LH, Turek FW, Takahashi JS. (1994) Mutagenesis and mapping of a mouse gene, *Clock*, essential for circadian behavior. *Science* **264**:719-25.

7 King DP, Zhau Y, Sangoram AM, Wilsbacher LD, Tanaka M, Antoch MP, Steeves TD, Vitaterna MH, Kornhauser JM, Lowrey PL, Turek FW, Takahashi JS. (1997) Positional cloning of the mouse circadian *Clock* gene. *Cell* **89**:641-53.

8 King DP, Vitaterna MH, Chang AM, Dove WF, Pinto LH, Turek FW, Takahashi JS. (1997) The mouse *Clock* mutation behaves as an antimorph and maps within the W^{19H} deletion, distal of *Kit*. *Genetics* **146**:1049-60.

9 Vitaterna MH, Ko CH, Chang AM, Buhr ED, Fruechte EM, Schook A, Antoch MP, Turek FW, Takahashi JS. (2006) The mouse *Clock* mutation reduces circadian pacemaker amplitude and enhances efficacy of resetting stimuli and phase-response curve amplitude. *Proc. Natl. Acad. Sci. U. S. A.* **103**:9327-32.

10 de Groot MH, Rusak B. (2004) Housing conditions influence the expression of food-anticipatory activity in mice. *Physiol. Behav.* **83**:447-57.

11 Barrett RK, Takahashi JS. (1995) Temperature compensation and temperature entrainment of the chick pineal cell circadian clock. *J. Neurosci.* **15**:5681–92.

12 Zheng B, Albrecht U, Kaasik K, Sage M, Lu W, Vaishnav S, Li Q, Sun ZS, Eichele G, Bradley A, Lee CC. (2001) Nonredundant roles of the *mPer1* and *mPer2* genes in the mammalian circadian clock. *Cell* **105**:683-94.

13 Bae K, Jin X, Maywood ES, Hastings MH, Reppert SM, Weaver DR. (2001) Differential functions of *mPer1*, *mPer2*, and *mPer3* in the SCN circadian clock. *Neuron* **30**:525-36.

14 Shearman LP, Jin X, Lee C, Reppert SM, Weaver DR. (2000) Targeted disruption of the mPer3 gene: subtle effects on circadian clock function. *Mol. Cell Biol.* **20**:6269-75.

15 Thresher RJ, Vitaterna MH, Miyamoto Y, Kazantsev A, Hsu DS, Petit C, Selby CP, Dawut L, Smithies O, Takahashi JS, Sancar A. (1998) Role of mouse cryptochrome blue-light photoreceptor in circadian photoresponses. *Science* **282**:1490-94.

16 van der Horst GT, Muijtjens M, Kobayashi K, Takano R, Kanno S, Takao M, de Wit J, Verkerk A, Eker AP, van Leenen D, Buijs R, Bootsma D, Hoeijmakers JH, Yasui A. (1999) Mammalian *Cry1* and *Cry2* are essential for maintenance of circadian rhythms. *Nature* **398**:627-30.

17 Vitaterna MH, Selby CP, Todo T, Niwa H, Thompson C, Fruechte EM, Hitomi K, Thresher RJ, Ishikawa T, Miyazaki J, Takahashi JS, Sancar A. (1999) Differential regulation of mammalian *Period* genes and circadian rhythmicity by cryptochromes 1 and 2. *Proc. Natl. Acad. Sci. U. S. A.* **96**:12114-19.

18 Debruyne JP, Noton E, Lambert CM, Maywood ES, Weaver DR, Reppert SM. (2006) A clock shock: mouse CLOCK is not required for circadian oscillator function. *Neuron* **50**:465-77.

19 Van den Pol AN. (1980) The hypothalamic suprachiasmatic nucleus of rat: intrinsic anatomy. *J. Comp. Neurol.* **191**:661-702.

20 Ralph MR, Foster RG, Davis FC, Menaker M. (1990) Transplanted suprachiasmatic nucleus determines circadian period. *Science* **247**:975-78.

21 Sujino M, Masumoto KH, Yamaguchi S, van der Horst GT, Okamura H, Inouye ST. (2003) Suprachiasmatic nucleus grafts restore circadian behavioral rhythms of genetically arrhythmic mice. *Curr. Biol.* **13**:664-68.

22 Welsh DK, Logothetis DE, Meister M, Reppert SM. (1995) Individual neurons dissociated from rat suprachiasmatic nucleus express independently phased circadian firing rhythms. *Neuron* **14**:697-706.

23 Yoo SH, Yamazaki S, Lowrey PL, Shimomura K, Ko CH, Buhr ED, Siepka SM, Hong HK, Oh WJ, Yoo OJ, Menaker M, Takahashi JS. (2004) PERIOD2::LUCIFERASE real-time reporting of circadian dynamics reveals persistent circadian oscillations in mouse peripheral tissues. *Proc. Natl. Acad. Sci. U. S. A.* **101**:5339-46.

24 Lucas RJ, Freedman MS, Lupi D, Munoz M, David-Gray ZK, Foster RG. (2001) Identifying the photoreceptive inputs to the mammalian circadian system using transgenic and retinally degenerate mice. *Behav. Brain Res.* **125**:97-102.

25 Provencio I, Rollag MD, Castrucci AM. Photoreceptive net in the mammalian retina. This mesh of cells may explain how some blind mice can still tell day from night. *Nature* **415**:493.

26 Hattar S, Liao HW, Takao M, Berson DM, Yau KW. (2002) Melanopsin-containing retinal ganglion cells: architecture, projections, and intrinsic photosensitivity. *Science* **295**:1065-70.

27 Shearman LP, Zylka MJ, Weaver DR, Kolakowski LF Jr, Reppert SM. (1997) Two *period* homologs: circadian expression and photic regulation in the suprachiasmatic nuclei. *Neuron* **19**:1261-69.

28 Shigeyoshi Y, Taguchi K, Yamamoto S, Takekida S, Yan L, Tei H, Moriya T, Shibata S, Loros JJ, Dunlap JC, Okamura H. (1997) Light-induced resetting of a mammalian circadian clock is associated with rapid induction of the *mPer1* transcript. *Cell* **91**: 1043-53.

29 Takumi T, Matsubara C, Shigeyoshi Y, Taguchi K, Yagita K, Maebayashi Y, Sakakida Y, Okumura K, Takashima N, Okamura H. (1998) A new mammalian *period* gene predominantly expressed in the suprachiasmatic nucleus. *Genes Cells* 3:167-76.

30 Albrecht U, Zheng B, Larkin D, Sun ZS, Lee CC. (2001) *MPer1* and *mper2* are essential for normal resetting of the circadian clock. *J. Biol. Rhythms* **16**:100-04.

31 Zylka MJ, Shearman LP, Weaver DR, Reppert SM. (1998) Three period homologs in mammals: differential light responses in the suprachiasmatic circadian clock and oscillating transcripts outside of brain. *Neuron* 20:1103-10.

32 Antoch MP, Song EJ, Chang AM, Vitaterna MH, Zhao Y, Wilsbacher LD, Sangoram AM, King DP, Pinto LH, Takahashi JS. (1997) Functional identification of the mouse circadian *Clock* gene by transgenic BAC rescue. *Cell* **89**:655-67.

33 Hubbard TJP *et al.* Ensembl 2007. Release 43. Feb 2007. *Nucleic Acids Res.* <www.ensemble.org>

34 Muller HJ. (1932) Further studies on the nature and causes of gene mutations. Sixth International Congress of Genetics, Ithaca, NY, Brooklyn Botanic Gardens, pp. 213-55.

35 Papp AC, Pinsonneault JK, Cooke G, Sad W. (2003) Single Nucleotide Polymorphism Genotyping Using Allele-Specific PCR and Fluorescence Melting Curves. *BioTechniques* **34**:2-6.

36 Turek FW, Joshu C, Kohsaka A, Lin E, Ivanova G, *et al.* (2005) Obesity and metabolic syndrome in circadian *Clock* mutant mice. *Science* **308**:1043-1045.

37 Kaasik K, Lee CC. (2004) Reciprocal regulation of haem biosynthesis and the circadian clock in mammals. *Nature* **430**:467-471.

38 Fu L, Patel MS, Bradley A, Wagner EF, Karsenty G (2005) The molecular clock mediates leptin-regulated bone formation. *Cell* **122**:803-815.

39 Antoch MP, Kondratov RV, Takahashi JS. (2005) Circadian clock genes as modulators of sensitivity to genotoxic stress. *Cell Cycle* **4**:901-7.

40 Hui E K-W, Wang P-C, Loa SJ. (1998) Strategies for cloning unknown cellular flanking DNA sequences from foreign integrants. *Cell Mol. Life Sci.* **54**:1403-11.

41 Shimomura K, Menaker M. (1994) Light-induced phase shifts in *tau* mutant hamsters. *J. Biol. Rhythms* **9**:97-110.

42 Sokolove PG, Bushell WN. (1978) The chi square periodogram: Its utility for analysis of circadian rhythms. *J. Theor. Biol.* **72**:131-160.

43 Abraham D, Dallmann R, Steinlechner S, Albrecht U, Eichele G, Oster H. (2006) Restoration of Circadian Rhythmicity in Circadian Clock-Deficient Mice in Constant Light. *J. Biol. Rhythms* **21**:169-176.

44 Bunger MK, Wilsbacher LD, Moran SM, Clendenin C, Radcliffe LA, et al. (2000) Mop3 is an essential component of the master circadian pacemaker in mammals. *Cell* **103**:1009-17.

45 DeBruyne JP, Weaver DR, Reppert SM. (2007) CLOCK and NPAS2 have overlapping roles in the suprachiasmatic circadian clock. *Nat. Neurosci.* **10**:543-5.

46 Zhou YD, Barnard M, Tian H, Li X, Ring HZ, Francke U, Shelton J, Richardson J, Russell DW, McKnight SL. (1997) Molecular characterization of two mammalian bHLH-PAS domain proteins selectively expressed in the central nervous system. *Proc. Natl. Acad. Sci. U. S. A.* **94**:713-8.

47 Reick M, Garcia JA, Dudley C, McKnight SL. (2001) NPAS2: an analog of clock operative in the mammalian forebrain. *Science* **293**:506-9.

48 Hong HK, Chong JL, Song W, Song EJ, Jyawook AA, Schook AC, Ko CH, Takahashi JS. (2007) Inducible and reversible Clock gene expression in brain using the tTA system for the study of circadian behavior. *PLoS Genet.* **3**:e33.